DESIGN AND FABRICATION OF MICROFLUIDIC PHOTOELECTROCHEMICAL REACTORS FOR EFFICIENT CONVERSION OF CARBON DIOXIDE TO LIQUID FUEL

by

HOMAYON HOMAYONI

Presented to the Faculty of the Graduate School of
The University of Texas at Arlington in Partial Fulfillment
of the Requirements
for the Degree of

DOCTOR OF PHILOSOPHY

THE UNIVERSITY OF TEXAS AT ARLINGTON

December 2014

To my parents.

ACKNOWLEDGEMENTS

I would like to express my gratitude to my advisor, Dr. Brian Dennis, for the opportunity he provided me to work on this dissertation. I would like to thank Dr. Rajeshwar, who let me use Electrochemistry lab equipment, Dr. Tacconi, Dr. Chanmanee, and Dr. Smuts for their technical support.

I would also like to acknowledge Dr. Kent Lawrence, Dr. Bo Ping Wang, Dr.Ratan Kumar, and Dr. Donhyun Shin for kindly accepting for serving on my Ph.D committee. Their advice and assistance are greatly appreciated.

I would like to thank all my lab members in CREST lab, who as good friends, was always willing to help me.

I would also like to thank my parents and my sister. They were always supporting me and encouraging me with their best wishes.

November 21, 2014

ABSTRACT

DESIGN AND FABRICATION OF MICROFLUIDIC PHOTOELECTROCHEMICAL REACTORS FOR EFFICIENT CONVERSION OF CARBON DIOXIDE TO LIQUID FUEL

Homayon Homayoni, Ph.D.

The University of Texas at Arlington, 2014

Supervising Professor: Brian H. Dennis

The worlds energy demand is expected to increase dramatically over the next few decades. At the same time the availability of cheap fossil fuels is expected to decrease. In addition to the increase in energy cost, the use of fossil fuels results in the release of greenhouse gases into the atmosphere. A lot research effort has been invested in the development of renewable energy resources that are cost competitive, sustainable, and emission free. Although these renewable technologies are available, many are not implemented widely due low efficiency and high capital cost. Therefore, fossil fuels are expected to remain a major source of the worlds energy for several decades. The release of carbon dioxide by the burning of fossil fuels is particularly problematic as these emissions are believed by many scientists to be the cause of global warming. To solve this climate change challenge, many researchers believe the carbon dioxide levels in the atmosphere should be reduced. One approach to this problem

is to employ methods that convert carbon dioxide into useful liquid or solid chemicals.

It has been known for decades that a mixture of carbon dioxide and water can be converted to useful liquids such as acids and alcohols via thermo/electro/photo-chemical methods. The electro and photo chemical approaches have resulted in liquid products with low carbon numbers, such as methanol and formic acid, using catalysts composed of Ruthenium, Palladium, Titanium oxides, and Copper oxides. Alcohols have a high fuel value and are arguably most important product of electrochemical reduction of carbon dioxide. The reported Faradic efficiency of alcohols is not high and the few cases with good Faradic efficiency the production rate and energy efficiency is low. Besides these low efficiencies, the price of some the catalysts are too high to be considered for industrial scale production. In an effort to increase the energy efficiency, this work employs a hybrid photo-electrochemical approach that uses solar energy to reduce the electricity required for carbon dioxide reduction to liquids.

A photo-electrochemical microreactor was developed to demonstrate this approach. This micro design increases the energy efficiency by decreasing the Ohmic losses while increasing production rates by improving mass transport of the reactants to the electrode surface. A novel nanostructured copper oxide surface is used as a semiconductor photoelectrode in this micro photo-electrochemical cell. Since the photoelectrode is produced from copper, an earth abundant element, it is more economical for industrial applications. The developed reactor has produced alcohols up to three carbons with high Faradic efficiency, which is novel and not reported by other researchers.

TABLE OF CONTENTS

LIST OF ILLUSTRATIONS

LIST OF TABLES

CHAPTER 1

INTRODUCTION

Hydrocarbons are used as fuel and raw material in various fields, including the chemical, petrochemical, plastics, and rubber industries. Despite their wide application and high demand, the need for alternative energy sources is becoming over more important with the rising costs of crude oil and the inevitable reality of peak oil. The recycling of environmental carbon dioxide by subsequent conversion to fuel would result in neutral carbon dioxide emissions by the fuel. This would not only be of interest based on cost of carbon dioxide, but it would also reduce the impact it has on global warming carbon dioxide, however, has been shown very little attention by industry and academia because of its high thermodynamic stability and having too high of an energy barrier for polymerization, even in presence of a catalyst.

1.1 Carbon Dioxide Emission

The level of the carbon dioxide emission in different regions strangely depends to stages of economic development as well as the dominate type of energy used [2]. Although developing nations have a less portion of world economy, they have more carbon dioxide emissions will be driven by these nations. The developing countries emissions will be raised about 50 percent by 2040, but the energy demand rises by about two-thirds. On the other hand the developed countries will be able to decrease this emission approximately 25 percent. It means the global mission of developing countries will shrink down from 40 percent in 2010 to 25 percent share of global emissions. It is interesting to know developed countries had 60 percent of global

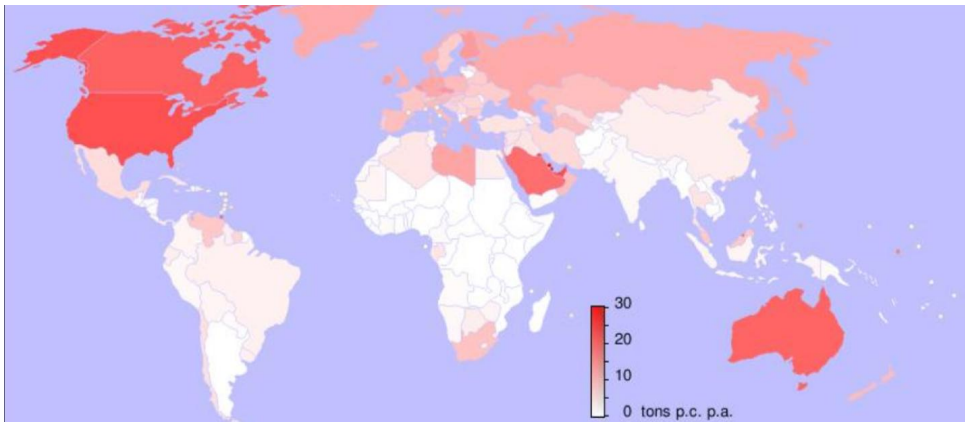

Figure 1.1. Carbon dioxide emission per capita per year per country [1].

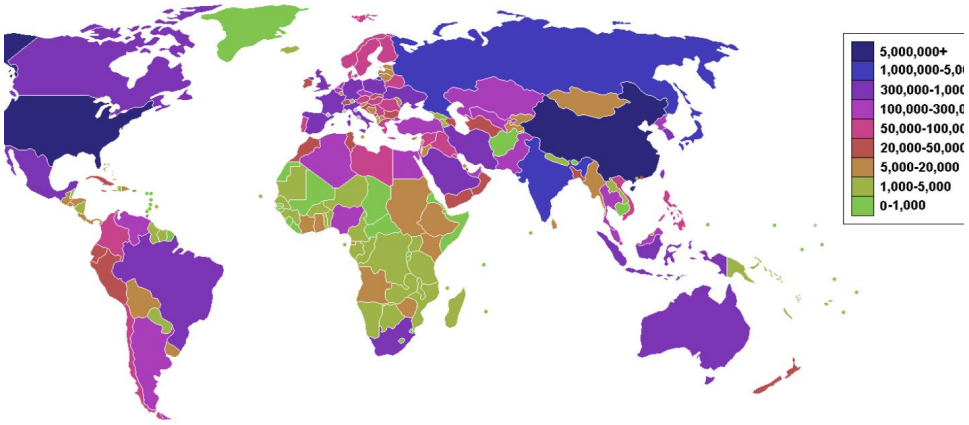

Figure 1.2. Countries by carbon dioxide emissions in thousands of tonnes per annum, via the burning of fossil fuels [1].

emissions back to 1980. The dioxide emission per person for different countries are presented in figure 1.1. Also the total carbon emission for these countries are presented in figure 1.2.

Figure 1.3 also shows the trend of carbon emission per capita from 2010 to 2040. Figure 1.4 shows the increasing the carbon dioxide in atmosphere in PPM. Because fossil fuels are the most demanded energy by human, carbon dioxide, the most dominate greenhouse gas emitted to air based on human activities, increases,

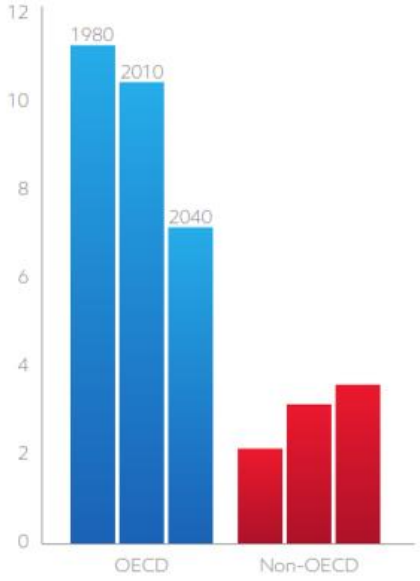

Figure 1.3. Energy related carbon dioxide emission, Tonnes per capita [2].

figure 1.5. To solve this climate change challenge reduction of carbon dioxide has been investigated by many researchers.

1.2 Climate change

One of the direct effect of high emission of carbon dioxide is the climate change [13, 14, 15]. This climate change has different signs and these signs varies from place to place. For instant for most of the U.S. it causes more harsh weather events, like, sustained summer heat, droughts, and winter storms. The hot and long summer in Texas in 2011, California drought in 2014, and the harsh winter storm in 2014 that happened nationwide are some of the recent evidence of this climate change. In U.S. annual average of the temperatures typically have been higher than the long-term average, in two last decades and summer average of temperature were above average for 12 of the last 14 summers [16].

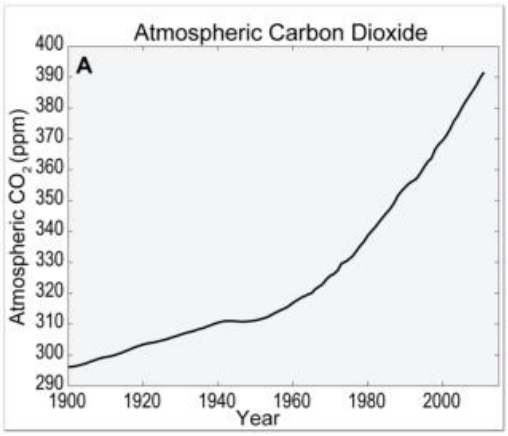

Figure 1.4. Carbon dioxide level of air [3].

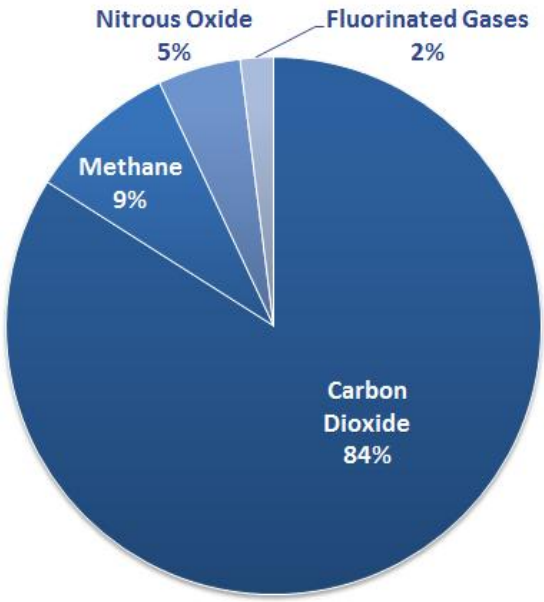

Figure 1.5. Carbon dioxide is the primary greenhouse gas emitted through human activities.

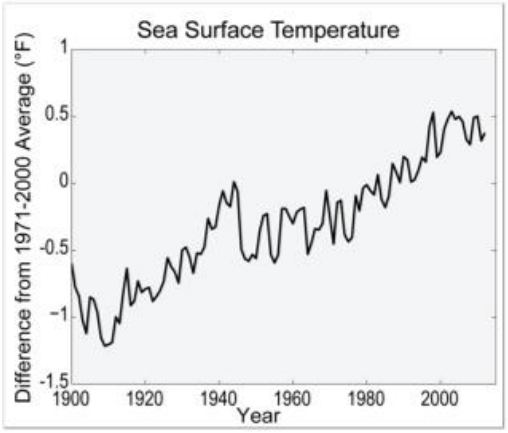

Figure 1.6. Increasing in sea water temperature [3].

Oceans also are affected by climate change. Water has a high heat capacity and because of it, oceans has a critical role in the Earths climate system. It is obvious that even small temperature change in such a huge water resource can have a large impact in ocean heat storage [17]. Sea surface temperatures in the North Atlantic and Pacific have started to increase since 1900 [18, 19]. This water temperature increase also has an impact on biological productivity in, because of increasing low oxygen zone in deep water oceans [11]. The temperatures of water surface for the ocean surrounding the U.S. have warmed by more than 0.9 over the past century figure 1.6. Oceans also have a huge impact to control of carbon emission by absorbing around a quarter of carbon dioxide emitted to air by human activity. This carbon dioxide, solved in water, increases the acidic property of sea waters [20, 21]. Surface ocean pH has declined by 0.1 units, figure 1.7, it means ocean acidity has been increased 30%, since preindustrial times [22].

This much increasing in ocean acidity has a damaging effect in ocean biological productivity. This acidic media causes repercussions creation in the marine food chain. For instance formation of calcium carbonate shells is more difficult in such

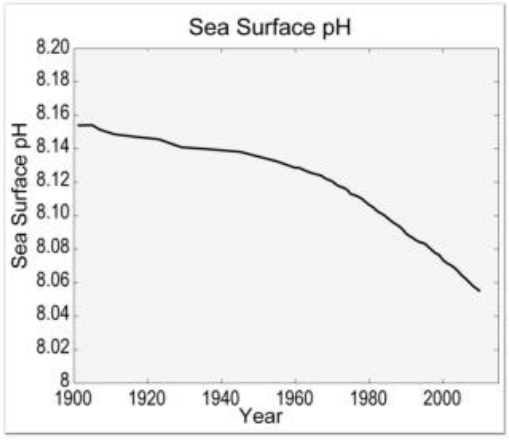

Figure 1.7. Increasing acidic behavior of sea water, decreasing in pH [3].

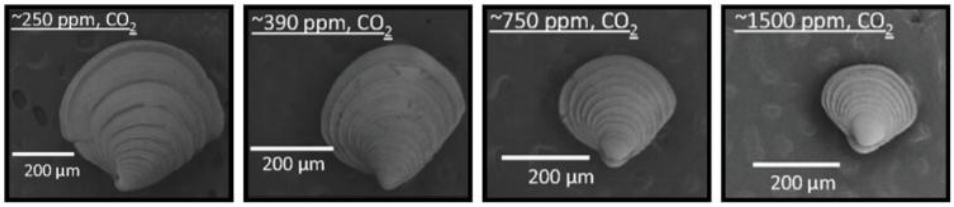

Figure 1.8. Shrinking in the size of clams in acidic water [4].

an acidic media. This calcium carbonate is the main skeletal component of various organisms in the oceans[23]. Shrinking in the size of clams in acidic water is presented in figure 1.8 [4]

1.3 Energy demand

The world energy demand increases dramatically over the next few decades, figure 1.9, and on the other hand fossil fuels resources as the primary human energy

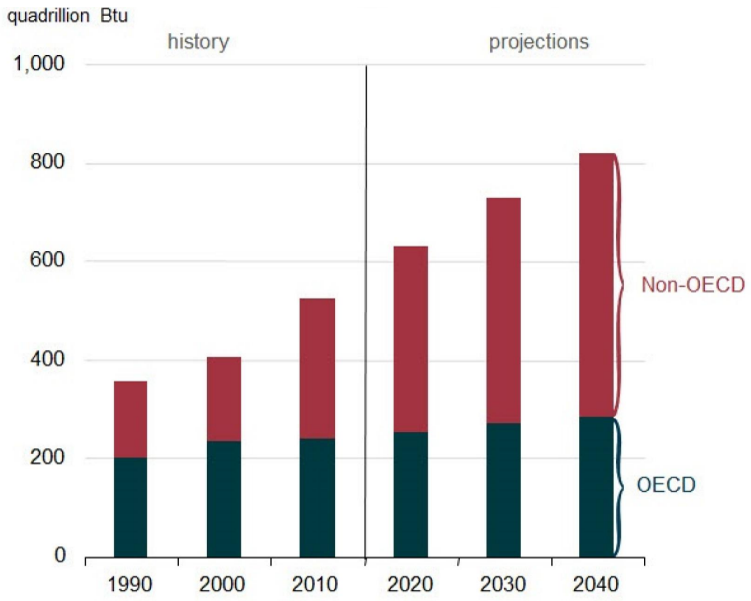

Figure 1.9. World Total Energy Consumption 1990-2040 (Source EIA).

source decrease, figure 1.10, sharply. By 2040 around 65% of words crude oil will be consumed, figure 1.11 [2].

To address the above mentioned problem in the few last decades some renewable energies have been introduced and applied as the sustainable energy, but due to the low efficiency and the high capital cost, still fossil fuels are the most demanded energy by human, figure 1.12. In future other source of liquid fuels will be produced more, but still crude oil usage will be more than 65% of all liquid fuels. It should be mentioned this percentage in North America will be around 20% [2] figure 1.13.

The mentioned increased temperatures, in the climate change section, also has effect on energy demand. For instance demand for energy to cool buildings will increase in long summers. As it has been mentioned earlier the average of the temperatures have increased in recent decades. This increasing has had an impact on energy demand. It has been reported that the negative effect of temperature incensement for 3degree Celsius, above preindustrial levels, will induce annual additional damages of

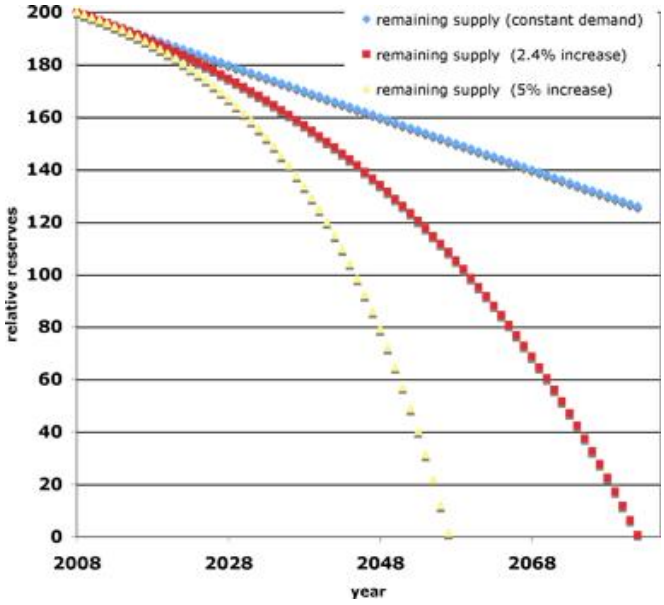

Figure 1.10. Projection of world fossil fuel resources.

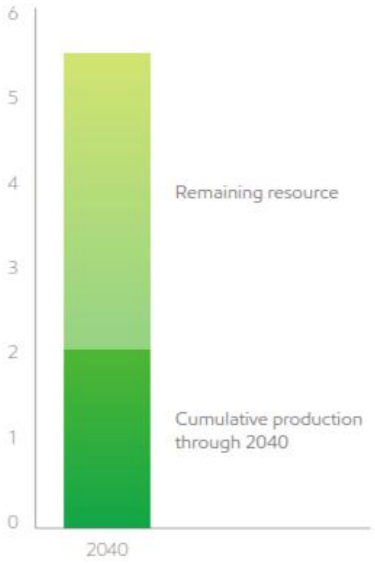

Figure 1.11. Crude oil and condensate resource (Source IEA).

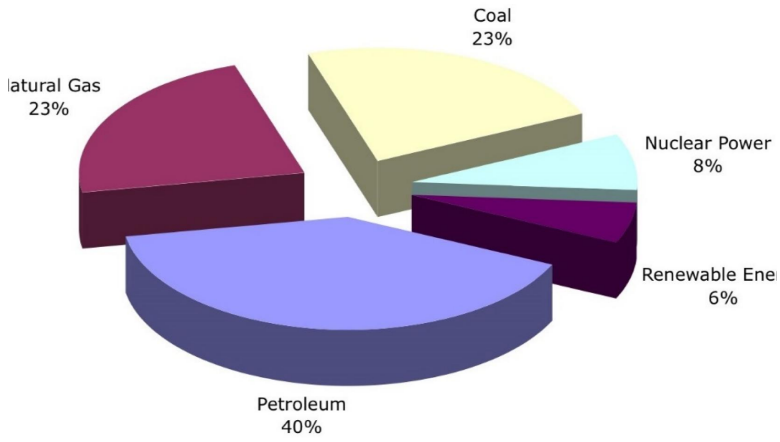

Figure 1.12. 86% US Energy concussion is Fossil fuel.

approximately 0.9 percent of global output [5]. Figure 1.14 illustrates this report. The next degree increase, from 3 to 4 degree Celsius, could cause more financial damage. This one degree increase costs of approximately 1.2 percent of global output.

As also it has been reviewed in this chapter carbon emission, from fossil fuel, has damaging effect on environment and on the other hand fossil fuel resource are limited. Converting carbon dioxide to some products could be a successful conversion and it could be even better if the carbon dioxide can convert to some fuel. In this case on only some part of carbon dioxide will be used as the feedstock, instead of emitted to atmosphere, but also some fuel has been produced that can help to energy crisis in future.

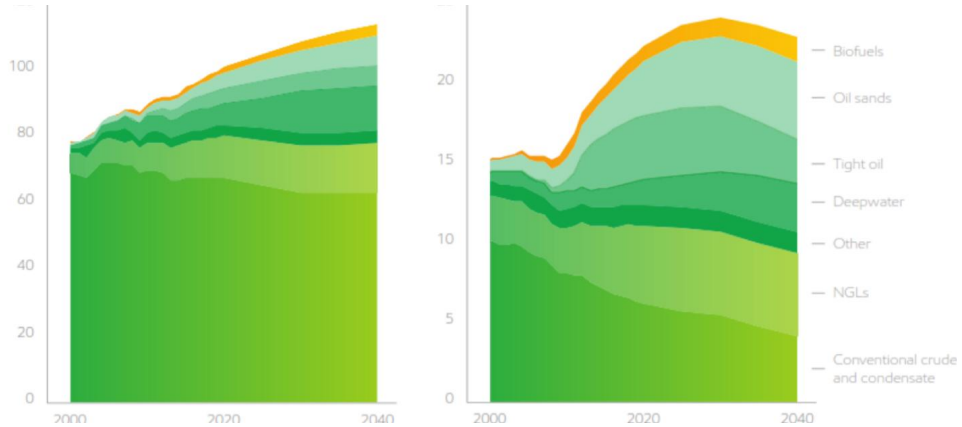

Figure 1.13. Liquids supply, global in left and North America in right. Millions of oil equivalent barrels per day capita [2].

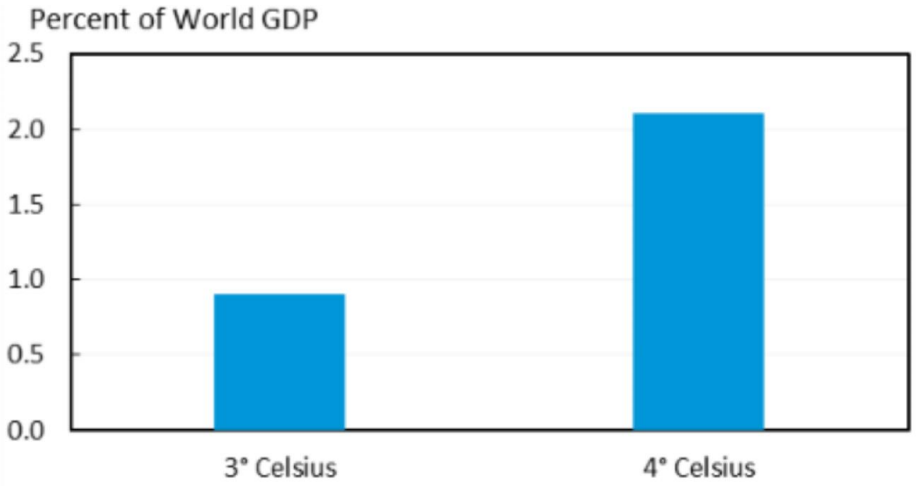

Figure 1.14. Economical damage from temperature increase more than 2° Celsius above the average [5].

CHAPTER 2

Literature review

The initial research to see the feasibility of the reduction of carbon dioxide in electrochemical cells initiated in ninth century [24, 25, 26, 27, 28] and in last few decades researchers have focused to produce desired products, with maximum efficiency by testing different electrolytes, working electrodes, counter electrodes, and cell designs in different temperatures and pressures.

In recent years, more research have been done regarding electrochemical reduction of carbon dioxide and this topic has taken more attention of researchers. This motivation comes from application of electrochemical reduction of carbon dioxide in different areas. Carbon dioxide can be electrochemically reduced to useful products under different conditions. For instance utilization of carbon dioxide [29, 30, 31] with new design of devices, synthesis of organic compounds like formic and oxalic acids for chemical industries usage [32, 33, 34, 35], and producing liquid fuel like methanol and ethanol as a potential energy source for future [36, 37, 38, 39]. However, the energy conversion efficiency, the ratio of the free energy of the products obtained in electrochemical carbon dioxide reduction and that consumed in the reduction, is roughly around 30 to 40% [38, 40]. This low efficiency could be discouraging to scale up the reduction of carbon dioxide [41].

Table 2.1. The Standard electrode potentials of the reduction of carbon dioxide in aqueous electrolyte at ambient temperature [12]

$$
\begin{aligned}
CO_2 + H_2O + 2e^- &= CO + 2OH^- && (-0.52\ V)\\
CO_2 + 6H_2O + 8e^- &= CH_4 + 8OH^- && (-0.25\ V)\\
2CO_2 + 8H_2O + 12e^- &= C_2H_4 + 12OH^- && (-0.34\ V)\\
2CO_2 + 9H_2O + 12e^- &= C_2H_5OH + 12OH^- && (-0.33\ V)\\
3CO_2 + 13H_2O + 18e^- &= C_3H_7OH + 18OH^- && (-0.32\ V)
\end{aligned}
$$

2.1 Products

The chemical reactivity of carbon dioxide is relatively low, but it needs to be highlighted that hydrogen evolution reaction (HER) in aqueous electrolyte solutions is also negative and close to the equilibrium potentials of carbon dioxide reduction. For instance the standard electrode potential of hydrogen evolution reaction (HER) at pH 7.0 at ambient temperature is 0.414 V and electrochemical reduction of carbon dioxide to formate ion in aqueous solution is 0.43 at same temperature and pH with respect to the standard hydrogen electrode (SHE). [41]

The Standard electrode potentials of the reduction of carbon dioxide in aqueous electrolyte at ambient temperature are presented in table 2.1 for formation of carbon monoxide, methane, ethane, ethanol, and Isopropanol. All of these values are estimated from thermodynamic data with respect to standard hydrogen electrode (SHE) [12]. The reduction of carbon dioxide has various product distributions. Metallic electrodes and the electrolyte solutions as well as temperature and pressure has effect on this product distribution. On the electrode surface different reactions happens, in parallel, so in most of the time there are various products with different faradic

efficiencies and the quantity of each product depends to the selectivity of the overall reaction which is affected by different conditions like electrodes, electrolyte solutions, temperature, pressure, pH, the currents density, and adsorption of reactants [41].

2.2 Electrodes and products

In term of selectivity in aqueous electrolytes, metal electrodes are divided into 4 main groups [41]. The first group has better selectivity to form formate. Pb, Hg, In, Sn, Cd, Tl, and Bi are metal electrodes in the first group. Formation of formate over Pb, Hg, In, Sn, and Cd as metal electrodes have been reported by many researchers [42, 43, 44, 45, 46, 47, 48, 49, 50, 51, 52, 53, 54, 55, 56, 57, 58, 59], also Tl [42, 43, 44, 45, 46, 47] and Bicite[60] have been mentioned as metal electrodes with selectivity to produce formate in other works.

Metal electrodes with better selectivity to make carbon monoxide are in the second group. Some metals like Au, Ag, Zn, Pd, and Ga. The best application of this group could be producing syngas. Formation of carbon monoxide have been reported over Au and Ag [42, 44, 45, 46, 47, 61, 62, 63, 64, 65, 66, 67, 68, 69, 70]. Zn and Pd not only can make carbon monoxide, but formation of formate also have been reported [42, 44, 45, 46, 61, 71, 72, 73, 74, 75, 76, 77, 78, 79]. The last member of this group is Ga with ability of carbon monoxide formation [80].

The third group is the most interesting group in the energy point of view. If some light hydrocarbon like methane and ethane or alcohols are desired products the Cu is the best metal electrode and it is the only member in the third group. Unlike formic acid and some other products, much less work have been done regarding electrochemical reduction of carbon dioxide to alcohols and only a few have reported good current efficiencies for methanol [81, 82, 83, 84, 85]. Formation of heavier alcohols like isopropanol, barely reported. Some of the reported research for hydrocarbon formation

Table 2.2. Hydrocarbon formation on some metal electrodes

Electrode	Products	References
Cu	CH_4, C_2H_4, C_2H_5OH	[41, 42, 44, 45, 46, 47, 48] [49, 50, 51, 52, 86, 87, 88] [89, 90, 91, 92, 93, 94, 95] [96, 97, 86, 87, 88, 89, 90] [91, 92, 93, 94, 95, 96, 97] [98, 99, 100, 101, 102, 103] [104, 105, 106, 107, 108, 109]
$Cu - Ni$	CH_4, C_2H_4, CO	[110]
Cu	CH_4, C_2H_4, CO	[111]
$Cu - Cd$	CH_4, C_2H_4, CO	[112]
$Cu - Au$	$CH_4, C_2H_4, EtOH, HCOO^-$	[113]
$Cu - Ag$	$C_2H_4, CO, CH_3CHO, C_2H_5OH$	[114, 115]
$Re - Ag$	CH_4, CO	[116]
$Ppy - Re - Au$	CH_4, CO	[117]
$Ppy - Re$	CH_4, CO	[118]

is presented in table 2.2, and some reported alcohols formation are presented on table 2.3.

For the fourth metal group only hydrogen evolution occurs and there is no any other product because of the reduction of carbon dioxide. This group includes Ni, Fe, Pt, and Ti. It needs to be highlighted these categories are valid only in ambient pressure. For instance some researchers have reported light Hydrocarbons formation such as methane, ethane and propane and even hydrocarbon with longer chain like isopropane and butane over metal electrodes in group four under pressure high pressure, 30 atm and 60 atm [119, 120].

Table 2.3. Alcohols formation on some metal electrodes

Electrode	Faradic Efficiency			References
	$MeOH$	$EtOH$	$PrOH$	
$Ru-GCE$	100			[49]
Mo	84			[51]
RuO_2/TiO_2	60			[118]
Ru	42			[45]
Cu/Ni	10			[40]
Cu		5.7	3	[118]
Pt		2.9		[118]

2.3 Electrolyte

Aqueous electrolyte has been the electrolyte in electrochemical reduction of carbon dioxide for a while, but recently, many researches have been done for electrochemical reduction of carbon dioxide using various metallic electrodes in organic solvents. Higher solubility of carbon dioxide in organic solvents is the main motivation replacing water with some organic solvent[121, 122, 122, 123, 124, 125].

For instance, in ambient temperature methanol can dissolve carbon dioxide about five times that water can dissolve [126, 127] and in subzero temperatures methanol dissolvability of carbon dioxide is eight to fifteen times more than water at [128]. Also In relatively low temperatures, methanol has been tested as catholyte for electrochemical reduction of carbon dioxide [129, 130]. In optimal experimental condition, the faradaic efficiency for methane, as the desired product, and the faradic efficiency of hydrogen, as a non-desired product, has been reported more than 42% and less than 8%, respectively [131].

Some products like oxalic acid, carbon monoxide, and formic acid have been reported as the main products by using organic solvent to reduce carbon dioxide, electrochemically over various metal electrodes [123, 124, 125, 132, 133].

Table 2.4. Hydrocarbon formation in the electrochemical reduction of carbon dioxide in methanol,with different salt at -30 degree Celsius

Salt	Faradic Efficiency			References
	CH_4	C_2H_4	$HCOOH$	
$LiCl$	68.4	4	6.8	[135]
$LiBr$	68.1	6.8	6.3	[135]
KBr	6.4	9.8	17.4	[136]
KI	15.8	19.9		[136]
$CsOH$	5.5	25.7	13.4	[137]
$LiOH$	58	16.5	6.8	[138]
$CsCl$	2.8	8.8	14.6	[139]

Some of the reports regarding hydrocarbon formation in the electrochemical reduction of carbon dioxide in methanol, as organic solvent, with different salt at -30 degree Celsius are presented in table 2.4[134, 135].

2.4 Pressure

Electrochemical reduction of carbon dioxide in ambient pressure in aqueous electrolytes and over metallic electrodes has been investigated by many researchers and electrocatalytic activities of different metallic electrodes have been reported. The effect of high pressure on electrochemical reduction of carbon dioxide also have been reported[140, 141, 50]. It is important to know product selectivity of electrochemical reduction of carbon dioxide chances substantially with increasing the pressure [142, 143, 144].

Positive effect of high pressure to produce formic acid and carbon monoxide by using optimal metallic electrodes via electrochemical reduction of carbon dioxide has been reported [145, 146]. For instance formic acid formed with a high Faradaic efficiency of 60% under high pressure, 30 bar, over Fe cathode [120]. Also formation

Table 2.5. Hydrocarbon formation in the electrochemical reduction of carbon dioxide in methanol over different electrodes at -30 degree Celsius

Electrode	Faradic Efficiency		
	CH_4	C_2H_4	C_2H_6
Cu	9.95	3.74	0.06
Fe	2.03	0.16	0.40
Ag	0.20		0.01
Au	0.21	0.11	0.02
Co	3.09	0.38	0.17
Rh	0.26	0.01	0.03
Ir	0.62	0.05	0.05
Zn	0.31		0.03

of methane has been reported under high pressure over Cu cathode at large current densities ($<$ 347 mA cm -2) [100]

Typically light Hydrocarbons such as methane, ethane and propane, are not easy to form electrochemically under 1 atm pressure over Fe, Co, and Ni. Better formation of these light hydrocarbon has been reported under high pressure. Also Fe, Co, and Ni as electrodes have been reported as capable cathodes to form some long chain hydrocarbons like Isopropane and butane, under pressure [120]. A summary of hydrocarbon formation of electrochemical reduction of carbon dioxide under high pressure is presented on table 2.5 [120, 121].

2.5 Temperature

The effect of temperature on the electrochemical reduction of carbon dioxide have been reported by researchers. Higher faradic efficiency has been reported with decreasing the temperature [47, 147, 148, 50]. This efficiency increase happens because of general decrease in hydrogen evolution. The first effect of temperature is

obvious. By decreasing the reaction temperature dissolvability of electrolytes is increased and it means there is more carbon dioxide ready to reaction and it would have leaded to higher faradic efficiency, if it was the only effect of the temperature increasing [149]. Changing temperature also has two more effects that make it more complicated [47, 147, 148, 150, 149, 151]. Increasing temperature causes to increase the mass transfer of carbon dioxide as well as increasing the exchange current density of the reaction. To separate these effects, solubility of carbon dioxide have been stabilized by adjusting the pressure [151] and electrochemical reduction of carbon dioxide has been reported in different temperature [151]. Hydrogen evolution has been reported significantly lower at lower temperatures for formation of formic acid.

This effect has been investigated in the other work for electrochemical reduction of carbon dioxide over Sn [134], but in constant pressure. To have the same amount of carbon dioxide in the electrolyte molar ratio of carbon dioxide has been adjusted. Higher Faradic efficiency for formic acid has been reported by increasing the temperature.

2.6 Cell design for Continues flow reactor

Li, H et al [149, 151] reported a new continues reactor for electro reduction of Carbon dioxide to Formic acid they used copper mesh as the cathode and reported 86% as thefaradic efficiency of Formate. Even 93% Faradic Efficiency for Formate has been reported by Subramanian et al Yamamoto, T et al [152, 153] for a reactor by using proton exchange membrane. worked on a continues reactor to make syngas out of Carbon Dioxide by using Gas diffusion Layer, GDL. They used carbon fiber for the cathode and nickel for the anode. Also Delacourt et al [154]. reported another continues reactor to reduce Carbon Dioxide to Syngas by without GDL. Also elec-

trolysis by using Solid Oxide in high temperature has been reported in several works [155, 156, 157] to make syngas. Alcohols as the major product has not been reported in any continues reactor up this date.

2.7 Solar and Semiconductor electrodes

In the late eighties, p-type photoelectrodes such as CdTe and GaP were reported for CO2 reduction in aqueous solutions [158]. Carbon monoxide and formic acid were the main formed products, the first dominating on p-CdTe while the latter was most favorable formed on p-GaP[158]. Latter on, p-GaAs and p-InP were deployed for methanol photogeneration but requiring very high overpotentials.[143] More recently, p-GaP and p-FeS2 photoelectrodes were showed to reduce carbon dioxide to methanol with the assistance of pyridine or imidazole in the electrolyte as cocatalyst [159, 160]. However, a drawback in several II-VI and III-V p-type semiconductor materials is that they are either toxic (As, Cd) or not earth abundant (Te, Ga, In).

Copper oxides exist in two forms, cuprous (Cu2O) and cupric (CuO) oxide with band gap energies of 2.0-2.2 eV and 1.3-1.6 eV respectively[161]. They are nontoxic p-type semiconductors, highly abundant and of much low cost than other II-VI and III-V semiconductor materials. Moreover, both oxides have conduction band-edges located negative enough to sustain carbon dioxide reduction [44] and additionally they have high absorption coefficients over a substantial portion of the solar spectrum.

No commercially available processes exist for the conversion of carbon dioxide to fuels and chemicals yet. The photoelectrocatalytic approaches have potentials to reduction of carbon dioxide to small carbon chain fuels. The semiconductor are ether toxic (As, Cd) or not earth abundant (Te, Ga, In) had been report to converting

carbon dioxide to liquid fuel. Some excellent review articles are summarizes the literature associated with carbon dioxide reduction different type of electrode material. Cu-based oxide is the only known material capable of catalyzing the formation of significant amount of hydrocarbon at high reaction rate over sustained period of time. Additionally copper oxides have high absorption coefficients over a substantial portion of the solar spectrum.

Methanol Faradaic efficiencies is reported up to 95% [162, 161] by showing that solar illumination of newly designed hybrid CuO-Cu2O nanorod arrays in a laboratory-scale photoelectrochemical cell, but the production rate is so low and the catalyst does not show a good stability. Methanol photogeneration was found to reach a concentration of about 85 μM after 90 min of radiation in batch two-compartment photoelectrochemical cell [162]. The yield of photoelectrosynthesis and selectivity can be changed substantially under different experiment condition such as concentration of the reactants, photoelectrocatalyst material, electrode potential, and temperature and electrolyte solution.

Now researchers face the challenge of implementing this type of chemistry on a large scale, designing a relatively inexpensive process that can compete successfully with current technologies. One of the major hurdles is coming up with a suitable design of the electrode and its reactor is a critical step for the feasible production of fuels from carbon dioxide on a large scale. Micro Reaction systems, in which the reaction occurs in channels or structures of critical dimensions in the range of m, may represent an interesting potential of features concentration the products and enhances detection. Compared to conventional reactors, a photoelectrochemical cell that includes a hybrid catalytic electrode with a large surface area and a small volume

of aqueous electrolyte solution formed products by applying a voltage to the cell as a stream of carbon dioxide flowed through it, the continuous flow system which enable considerable enhancement of mass transfer of carbon dioxide. The high surface-to-volume ratios resulting from the narrow reaction volumes significantly enhance current density and Faradaic efficiency. This may again allow for accommodation of catalysts with activity 1-2 orders of magnitude higher than conventional cell. Eventually, this could lead to increased product yields, improved energy efficiency, improve the activity and selectivity of the electrodes, and reduced capital costs.

CHAPTER 3

Electrochemistry

In this chapter some electerochamical definition have been reviewed. These definition will help to have a better understand of other chapters.

3.1 Electrochemical cell and standard half-cell potential

An electrochemical cell is a device to convert chemical energy via chemical reaction into electrical energy. If the electrochemical cell is used for this purpose it is also Voltaic cell or a Galvanic cell. In an electrochemical cell two reactions happens. Oxidation and reduction reactions are capable to provide electricity energy. This phenomena happens in batteries. In the electrochemical reaction oxidation happens on the anode side and released electrons go to the cathode side via the external circuit path. Using copper and zinc metals with solutions of their sulfates is a simple example of electrochemical cell components, figure 3.1.

If electrons move, which always move from anode to cathode, from positive potential to negative potential, electricity energy will be generated in the electrochemical cell or Voltaic cell in this case. If electrons move from negative to the positive potential, applying electricity is needed to make this movement in the electrochemical cell. This case is same as electrochemical cell for reduction of carbon dioxide. A net electrochemical reaction is performed in a complete cell. The anode electrodes oxidizes and the cathode electrode reduces reactants. These oxidation and reduction which occur on two different electrodes can be assumed occur in two half cells. These

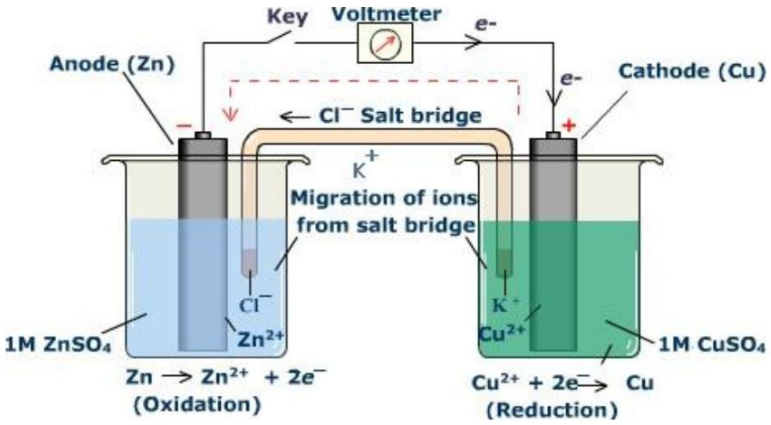

Figure 3.1. Voltaic Cell of zinc metals with solutions of their sulfates [6].

two half cells could be totally separated, but a salt bridge to make a close electric circuit is necessary. Figure 3.1 also shows an electrochemical cell with two half cells.

3.2 Salt bridge vs membrane

External electrical circuit between the two electrodes in an electrochemical cell makes it possible the cell works, but the two electrolytes need to have an electrical connection together, otherwise the electrochemical cell would be an open circuit. In order to having a close circuit, to make the chemical reaction possible, in order to sustain the cell reaction, the charge must be accompanied by a compensating transport of ions between the two electrodes, when electrodes are separated in two cells, gure3.2. By adding a salt bridge between two cells the circuit will be close. Salt bridge is a path for ions to move directly from one electrode to the other one.

If both electrodes are maintain in a same cell and separation of two side of electrolyte, catholyte and anolyte, is not needed, there is no need to use any salt bridge. Because in this case the circuit is already close. If both electrodes are in a same cell and to not let the products from one side go to the other side, separation

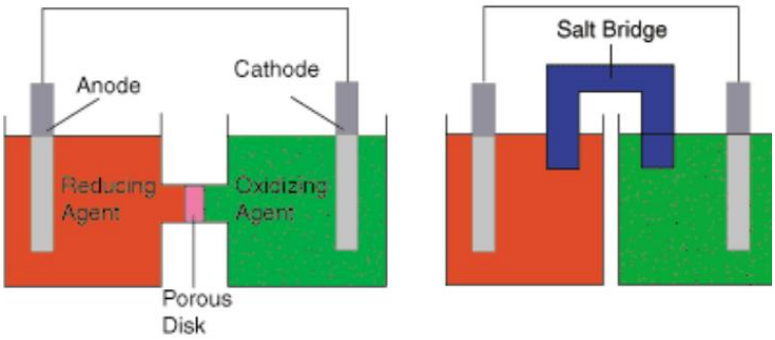

Figure 3.2. Two different type of salt bridges [7].

of two sides in necessary. In this case porous membrane can be used. These porous membrane come with different pore size.

3.3 Proton exchange membrane

A proton exchange membrane or ion exchange membrane works like a porous membrane with small thickness and with very small pore size. The preliminary application of solid polymer electrolyte (SPE), also referred to as the proton exchange membrane (PEM), are for electrolytes for fuel cells and water electrolysers. These membranes have very high thermal stability as well as high conductivity. High mechanical and chemical stability with very low permeability to gases are other unique properties of these membranes. The most common type of membrane, commonly used in fuel cell because of aforementioned properties, is Naon. Naon also has been used in this current work as the membrane in microfluidic photoelectrochemical reactors.

3.4 Fuel cell vs Electrochemical cell

In the fuel cell, the fuel is oxidized on the anode to protons as well as electrons. The protons go through electrolyte, with membrane, and the electrons can go through

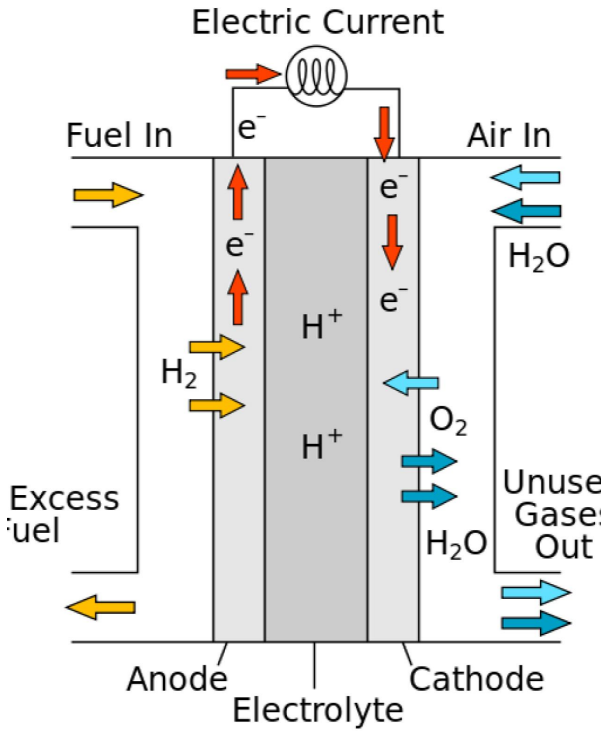

Figure 3.3. A schematic of a fuel cell [8].

an external electrical circuit. Those electrons are the source the electrical power. The protons passing through the electrolyte and membrane and electrons passing through the external circuit can react on the cathode with available oxygen. The result of this reaction is producing water in cathode side, figure 3.3.

On the other hand, in a carbon dioxide reduction cell, water is oxidized on the anode side, instead of oxidation of fuel in fuel cell. Protons and electrons are released because of this oxidation, again same as fuel cell protons go through the electrolyte and membrane and the electrons can through the external circuit. This time electrons move from the anode that has more positive potential to the cathode with more negative potential. This electron movement from positive to negative potential is not happened, but applying an external electric power. However the protons which went

through electrolyte and electrons which went through the external circuit can join together on the cathode side to reduce carbon dioxide and produce desired products.

3.5 The hydrogen evolution reaction (HER)

The electrochemical activity of hydrogen evolution reaction (HER) on dierent metals are on a so-called Vulcano plot, gure 3.4. On this plot the bond energy of chemisorbed Hydrogen atom to the metal is related to the exchange current [9]. As it is shown on the Vulcano plot the most active metals towards the hydrogen evolution reaction are metals of intermediate bond-strength energy [9]. The metals on the left side of the Vulcano plot are metals with low bond-strength and the metals on the right have stronger bond-strength the hydrogen [163]. Because noble metals have high corrosion resistance in acidic solution, these metals are reviewed more and they are presented on the Vulcano plot. The most active catalyst for the HER is platinum and it has wide application because of this property, but platinum high price of platinum is still a big problem for industries.

3.6 The oxygen evolution reaction (OER)

Acidic media is corrosive for many transition metals like Ni, Co, and Mn, but oxides of iridium or ruthenium can be still active catalysts in the same acidic media. The correlation of the catalytic activity versus the current are presented in Vulcano plots for the oxygen evolution reaction, figure 3.5. This Vulcano plot identifies the oxides of iridium or ruthenium as the most active catalyst towards the oxygen evolution reaction OER. The standard potential for the oxygen electrode is 1.23 V, but it goes above this standard potentials for many elements and only a few materials can be stable in acidic solution, like it was mentioned earlier. Also it should be mentioned

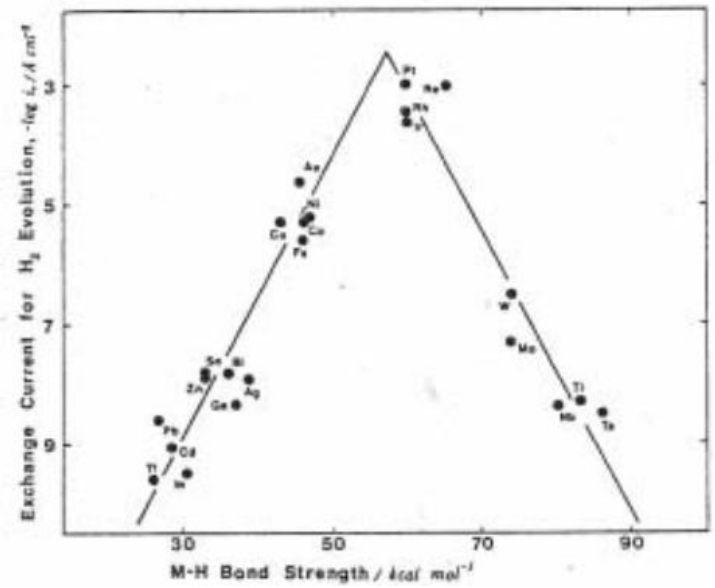

Figure 3.4. Vulcano plot of HER for different metals [9].

the oxygen evolution reaction is a complex reaction. The OER has different pathways of high activation energy and high energetic intermediates[164].

3.7 Reference Electrodes

Desired products of chemical reactions in electrochemical experiments are produced on surface of electrodes and based on our desired products, these products could be made on cathode electrode or anode electrode. The major motivation to using reference electrodes is keeping the right voltage needs to make the desired product on the surface of electrode. To measure the voltage in a complete cell involving two electrode systems, typically the reference electrode needs to be place in the half of the cell that desired products are produced. By doing this, the reference electrode can maintain the right voltage on the electrode surface and have the stable potential. The simplest reference electrode could be a metal wire with very low electric resistance, like gold or platinum. This metal wire could be inserted directly into the electrolyte

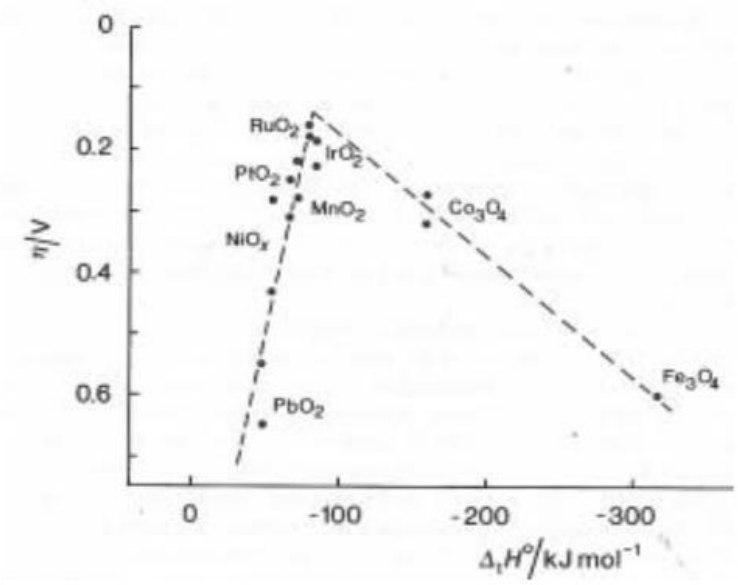

Figure 3.5. Overpotential at 0.1 mA.cm on dierent metal oxides as a function of enthalpy [10].

as close as possible to the surface of the electrode which is supposed to make the desired product. By having the reference electrode at close position to the electrode, having the exact and constant potential on the surface of electrode is possible. The other most common way of making a reference electrode is to use an electrode reaction involving a saturated solution of an insoluble salt of the ion. Figure 3.6 shows different type of reference electrodes.

3.8 Faradic efficiency

Faradic efficiency of a product is the portion of the charge (electrons) changed to desired product to all charge made in an electrochemical system. The unit for charge is the faraday, but it also could be presented by the coulomb. The equation 3.1 gives the faradic efficiency of methanol

$$\text{Faradic Efficiency of } MeOH = \frac{Num}{Den} \tag{3.1}$$

Figure 3.6. Different type of reference electrodes.

$$Num = 100 \times \text{Concenteration of } MeOH(\frac{\mu Mole}{Liter}) \times 10^{-6}(\frac{Mole}{\mu Mole})$$
$$6.02214129 \times 10^{23}(\frac{MeOH \text{ Molecules}}{Mole}) \times 6(\frac{\text{Electrons}}{MeOH \text{ Molecules}})$$
$$\frac{1}{1000}(\frac{Liter}{ml}) \times \text{Flow rate}(\frac{ml}{hr}) \times \frac{1}{3600}(\frac{hr}{s}) \tag{3.2}$$
$$Den = \text{Current } (mA) \times \frac{1}{1000}(\frac{A}{mA}) \times 6.24 \times 10^{18}(\frac{\text{Electrons}}{A} \times \frac{1}{s}) \tag{3.3}$$

3.9 Cyclic voltammetry (CV)

Cyclic voltammetry is a method to study the adsorption of different species in a reaction at the electrode surface. Cyclic voltammetry (CV) is a surface sensitive technique. This method typically is applied for determination of the physio-chemical state of an electrode surface. In Cyclic voltammetry current response is measured by sweptwing the potential for each rate in the inserted potential range. Coecients of electroactive species and the active surface area of electrodes, electrode capacitance, can be measured by cycling the potential at dierent scan rates. Some information

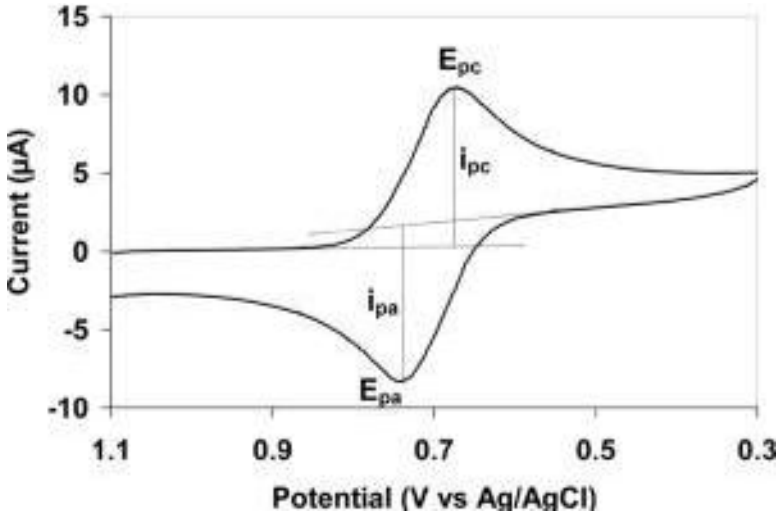

Figure 3.7. Typical cyclic voltammetry graph [11].

regarding with discharge presses and charge reversibility can be obtained with cyclic voltammetry (CV) [165]. Figure 3.7 shows the typical cyclic voltammetry result. By doing this test it will be clear in what potential, the electrochemical cell produce the maximum current.

CHAPTER 4

Experimental Section

To reduce Carbon dioxide to alcohols in this work three different types of microfluidic reactors have been made. The first one is Photoelectrochemical microfluidic reactor with three channels, the second one is electrochemical microfluidic reactor with two channels and the last one is Photoelectrochemical microfluidic reactor with two channels.

4.1 Microfluidic reactor design

4.1.1 Photoelectrochemical microfluidic reactor with three channels

A microfluidic reactor has been designed and fabricated with a large area photocathode in contact with flowing CO2-saturated electrolyte through microchannels to reduce Carbon dioxide. Compared to conventional reactors, this Photoelectrochemical microfluidic includes a hybrid copper oxide photoelectrode with a large surface area in contact with a small volume of aqueous electrolyte solution to form products under solar irradiation and low bias voltage. The CO2-saturated electrolyte is continuous flowing through microchannels which enable considerable enhancement of mass transfer of Carbon dioxide. For products photogeneration, the target was in fact the formation of liquid fuels with C$\geq$2 because they are easier to transport and store, preserving the large investments made in the current energy and chemical infrastructures [166]. As it is shown on the Figure 4.1 the electrolyte on the cathode side flows on the top of the cathode in the first channel and then flows underneath of the cathode in the second channel to the outlet where electrolyte can have contact

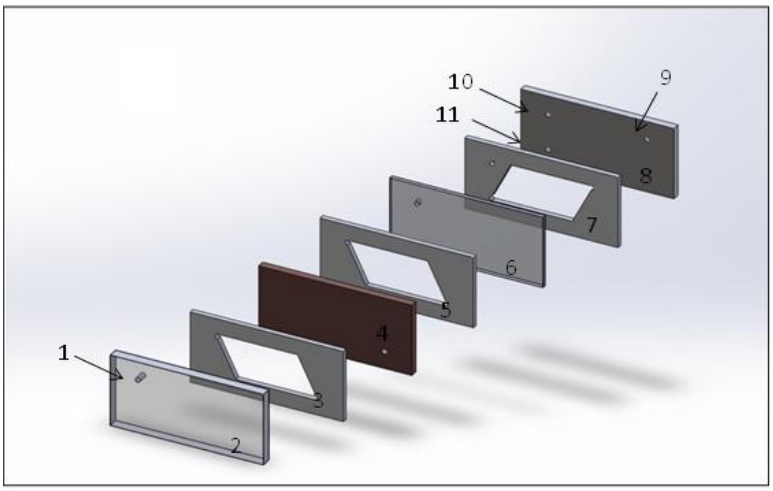

Figure 4.1. Scheme of the photomicroreactor (1) Catholyte inlet and the location of the reference electrode, (2) The transparent part, (3) Microchannel arrays on top of the cathode, (4) The cathode, (5) Microchannel arrays underneath the cathode, (6) The membrane, (7) Microchannel arrays on the anode, (8) The Anode, (9) outlet of anolyte, (10) outlet of catholyte, (11) inlet of anolyte.

with the membrane. On the anode side electrolyte flows in the third channel. A schematic of this Photoelectrochemical microfluidic is depicted in Figure 4.1. Figure 4.1.1 shows an image of a Photoelectrochemical microfluidic with three channels.

4.1.2 Electrochemical microfluidic reactor with two channels

This microfluidic reactor has been design for reduction of Carbon dioxide without solar energy and because of this in this microfluidic reactor there is no need to have a transparence part on the top of the cathode and it is possible to have a microfluidic reactor with two channels. A schematic of an electrochemical microfluidic reactor with two channels is shown in the figure 4.1.2.

As it is shown in Figure 4.1.2 there are channels in this micro rector, one for the anode side and one for the cathode side. In this design the cathode side is facing to the

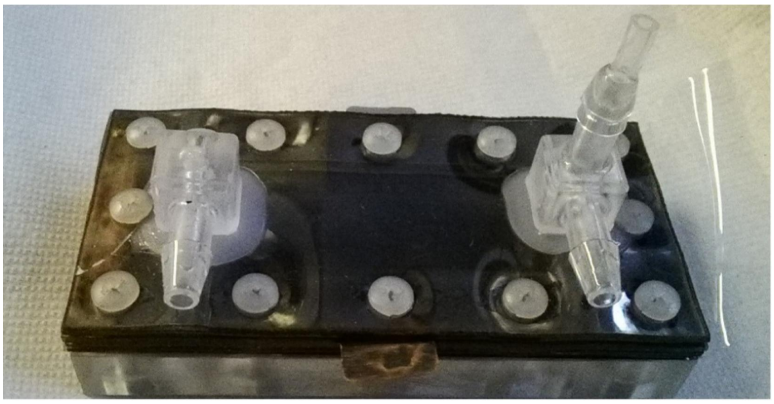

Figure 4.2. A Photoelectrochemical microfluidic whith three channels in it.

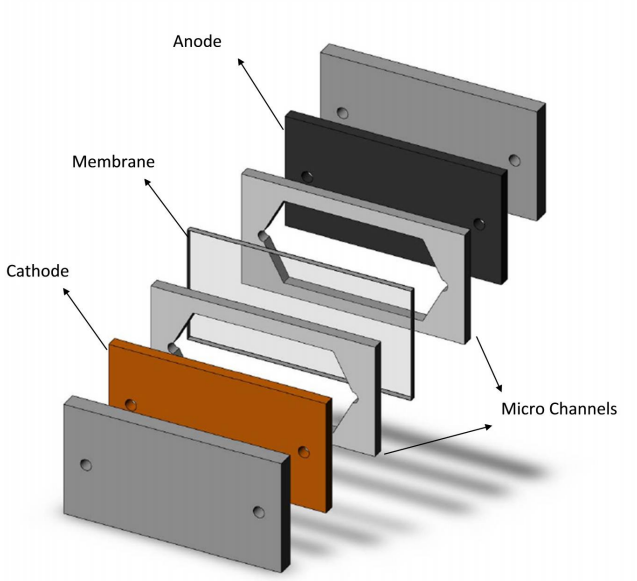

Figure 4.3. Schematic representation of an electrochemical microfluidic reactor with two channels.

membrane, but in the first design for reduction of Carbon dioxide with solar energy, a Photoelectrochemical microfluidic with three channels, the back side of the cathode is facing to the membrane and top side of the cathode is facing to the transparent part.

4.1.3 Photoelectrochemical microfluidic reactor with two channels

Not only fabricating a microfluidic reactor with two channels is easier and cheaper than fabricating microfluidic reactor with three channels and less material is needed, but also because of having only one channel on the cathode side instead of two there is less pressure drop for electrolyte on the cathode side. This less pressure is more important if a number of these microfluidic reactors are stacked up and the power which is required to make electrolyte flow on the cathode side decries dramatically. Also because of less layers used in a microfluidic reactor with two channels, this microfluidic reactor has a smaller thickness.

To have a microfluidic reactor with only two channels that can reduce Carbon dioxide photoelectrochemically, the third type of microfluidic reactor has been designed and fabricated. In design of the cathode electrode has been changed and three holes has been added on the cathode electrolyte, as it is shown in figure 4.1.3, these holes let the electrolyte on the cathode side has contact with the membrane when it flows on the first channel. The area of cathode electrode in this design is less than the first design, because of the three holes on the cathode surface, but instead this design is has smaller thickness, it is lighter because of less material used in this micro reactor and as it has been mentioned electrolyte has less pressure drop. An image of photoelectrochemical microfluidic reactor with two channels is shown in figure 4.1.3.

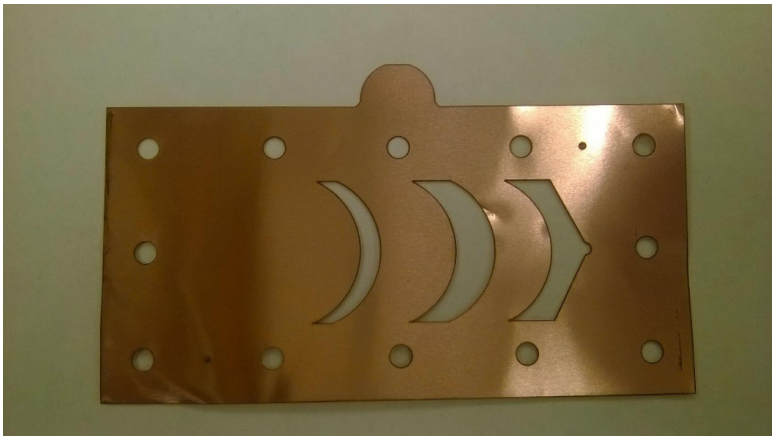

Figure 4.4. A cathode side in a photoelectrochemical microfluidic reactor with two channels.

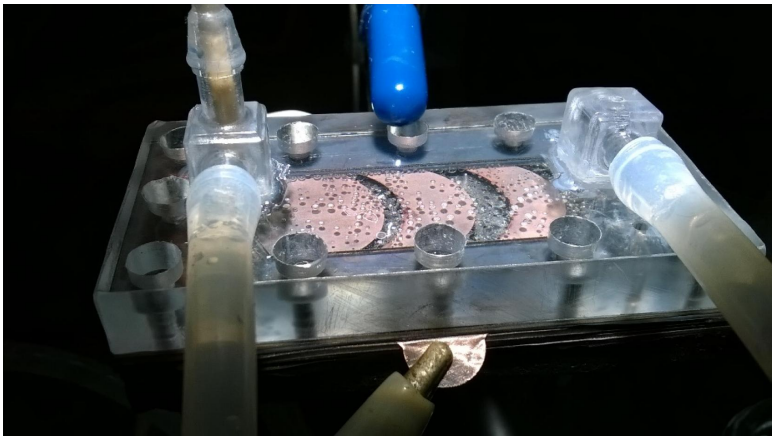

Figure 4.5. A photoelectrochemical microfluidic reactor with two channels in a electrochemical test.

4.2 Experimental setup

A schematic of the complete setup for photoelectrochemical conversion of Carbon dioxide to fuels with the third type of micro rector is shown in Figure 4.6 while the complete setup for and electrochemical conversion of Carbon dioxide to fuels via the second type of micro rector is depicted in Figure 4.7.

The supporting electrolyte was sodium bicarbonate (0.1 M) and was pumped to the membrane-based microchannel gas exchanger where the electrolyte became saturated with Carbon dioxide. The Carbon dioxide was delivered at 1 ATM from a pressurized tank at room temperature. Under these conditions, the maximum solubility of Carbon dioxid in water is 0.034 mol/L.10 A 35 ml syringe was used and 10 ml per hour was applied as the flow rate by a syringe pump (KD Scientific 200). Carbon dioxidsaturated electrolyte was then delivered to the cathode compartment located at the top of the microreactor and irradiated with sunlight (AM 1.5) from a solar simulator (New Port 91160). The reference electrode also was located at the input of the cathode side. Ag/AgCl was used as reference electrode and CuO/Cu2O hybrid nanorod arrays supported on a copper foil was placed in the cathode compartment. Then electrolyte was pushed underneath of the cathode (Figure 4.7), and cathode and anode compartments were separated with an ion-exchanger membrane and then collected through the sample collector. Stainless steel 378 (Trinity band industries,Inc) were used as the anode and Nafion NER-212 (Fuel cell Earth, USA) as ion-exchange membrane. Electrolyte for the anode side was pumped to the bottom of microreactor where the anode was located and then delivered to the anolyte collector. The anolyte flow rate was 5 to 10 ml per hour and provided by a metering pump (Control Company 3388). The experimental setup has been shown in figure 4.8.

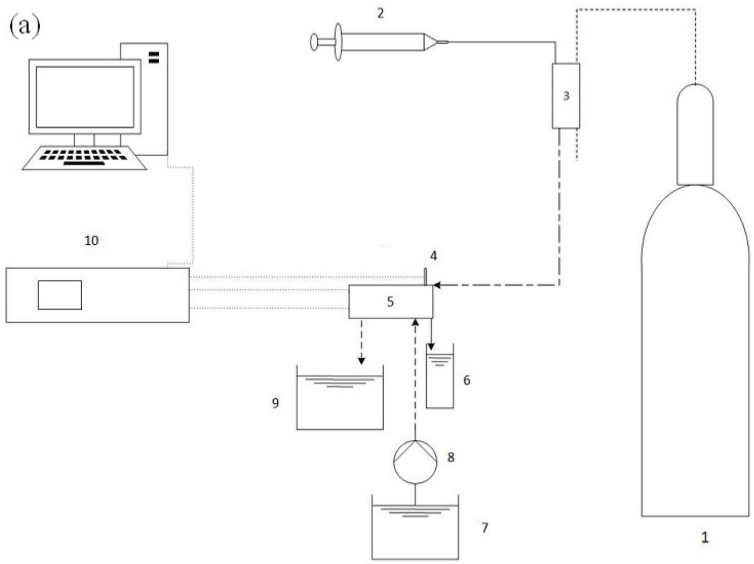

Figure 4.6. Schematic diagram of an experimental setup for a Microfluidic reactor (1) Carbon dioxide tank, (2) Syringe pump, (3) Membrane mass mixture, (4) Reference electrode, (5) Microreactor, (6) Solar simulator, (7) Fresh anolyte, (8) Pump, (9) Used anolyte, (10) Electrochemical work station.

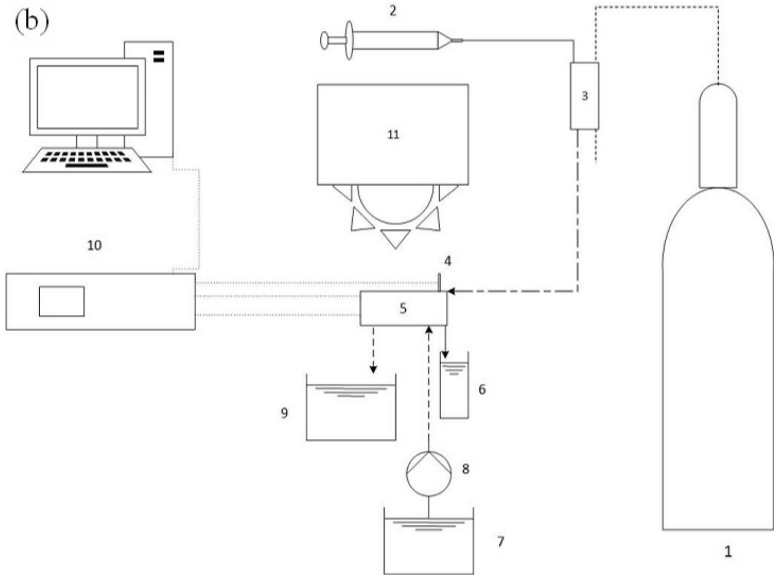

Figure 4.7. (b) Schematic diagram of experimental setup for the photomicrophotoreactor.(1) Carbon dioxide tank, (2) Syringe pump, (3) Membrane mass mixture, (4) Reference electrode, (5) Microreactor, (6) Solar simulator, (7) Fresh anolyte, (8) Pump, (9) Used anolyte, (10) Electrochemical work station, (11) solar simulator.

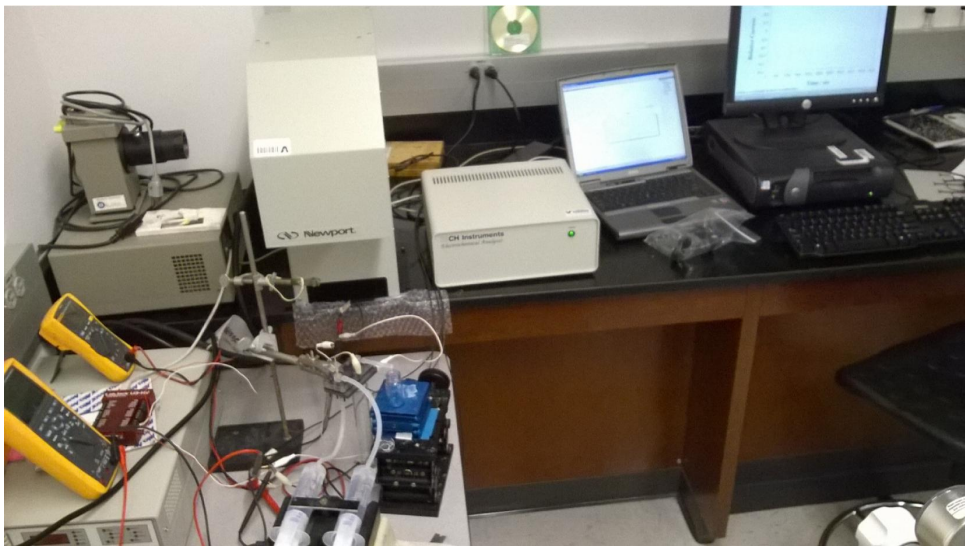

Figure 4.8. The experimental setup.

CHAPTER 5

Result and Discussion

In this chapter, results are presented in three sections. First how to make photo electrodes, photocathodes, then how to detect products and finally some sample results of photoelectrochemical microfluidic reactors and electrochemical microfluidic.

5.1 Photocathode

5.1.1 Introduction

As it was mentioned in chapter 2, in the late eighties, p-type photoelectrodes such as CdTe and GaP were reported for Carbon dioxide reduction in aqueous solutions[158], but Carbon monoxide and formic acid were the main formed products, the first dominating on p-CdTe while the latter was most favorable formed on p-GaP[158]. P-GaAs and p-InP were deployed to make methanol photo-chemically, but with very high overpotentials[167]. More recently, p-GaP and p-FeS2 photoelectrodes were shown to reduce carbon dioxide to methanol with the assistance of pyridine or imidazole in the electrolyte as co-catalyst [159, 160]. However, a drawback in several II-VI and III-V p-type semiconductor materials is that they are either toxic (As, Cd) or not earth abundant (Te, Ga, In). As it is mentioned, Copper oxides exist in two forms, cuprous (Cu2O) and cupric (CuO) oxide with band gap energies of 2.0-2.2 eV and 1.3-1.6 eV, respectively [161]. They are nontoxic p-type semiconductors, highly abundant and of much lower cost than other II-VI and III-V semiconductor materials. Moreover, both oxides have conduction band-edges located negative enough to sustain carbon dioxide reduction [44], and additionally, they have

high absorption coefficients over a substantial portion of the solar spectrum. The hybrid of cuprous (Cu2O) and cupric (CuO) oxide has been used in this work.

5.1.2 Photocathode preparation

The hybrid CuO/Cu2O nanorod arrays were fabricated by a two-step process performed on freshly cleaned copper. Briefly, the cleaning procedure consisted in pre-treating copper substrates with 1.0 M H2SO4 (Sigma-Aldrich), then subjecting them to successive sonication in isopropanol, acetone and deionized water, and finally, dry them under nitrogen gas. The first step, and at variance with our reported procedure for formation of CuO/Cu2O nanorod arrays [168, 162], consists in colloidal formation of Cu(OH)2 which are then transformed in CuO nanowire arrays. Thus, freshly cleaned Cu substrates were immersed in the mix solution 8.0 mL of the 10 M NaOH solution (Sigma-Aldrich), 4.0 mL of 1 M (NH4)2S2O8 solution (Sigma-Aldrich, 99.9% metals basis), and 18.0 mL of double-distilled water (Corning Megapure). A few minutes later, blue color appeared on the copper foil surface, and the solution became increasingly blue, as it is shown in figure 5.1. After a few minutes a light-blue film covered the copper foil surface. It is shown in figure 5.1 only after around two minutes, the color of the solution and the cooper foil start to change. Different soaking time make different size and morphology of nanowires. The copper foil was taken out of the solution, rinsed with water, and dried in air. The Cu(OH)2 fibers and scrolls were converted into CuO nanowires by thermal oxidation in the presence of air using a box furnace for 2 h. at 200 degree Celsius (at 10 degree per minute). The temperature was allowed to return naturally to room temperature. After this step, the copper foil color is turned to black. The whole procedure is labelled as CH τ where CH stands for the chemical formation of Cu(OH)2 during a time τ. As all films were then subjected to the same thermal treatment for conversion to CuO, no

Figure 5.1. Formation of Cu(OH)2 on Copper foils after around 2 minutes in the left beaker and fresh copper foil are just inserted in solution in the right beaker.

additional information is included in their labeling. Some copper foils after 2 hours of chemical oxidation in the oven have been shown in figure 5.2.

In the second step, Cu2O crystallites were electrodeposited on the just formed CuO by using constant potential in an electrolytic copper sulfate bath containing lactic acid [169, 170, 171, 172, 173, 174, 175].The electrolytic bath was prepared with deionized (DI) water and contained 0.4 M cupric sulfate (Sigma-Aldrich, 99.9% metals basis) and 3 M lactic acid (Sigma-Aldrich). The bath pH was adjusted to 9 by the addition of concentrated sodium hydroxide solution; the temperature of the bath was maintained at 60C during electrodeposition. A Pt foil and an Ag/AgCl (satd. KCl) were used as counter and reference electrode, respectively.

5.1.3 Morphology of different Photocathode

The morphology of the CuO nanowires, Cu2O crystals, and a hybrid of cuprous (Cu2O) and cupric (CuO) oxide vary with the soaking time in the first step as well

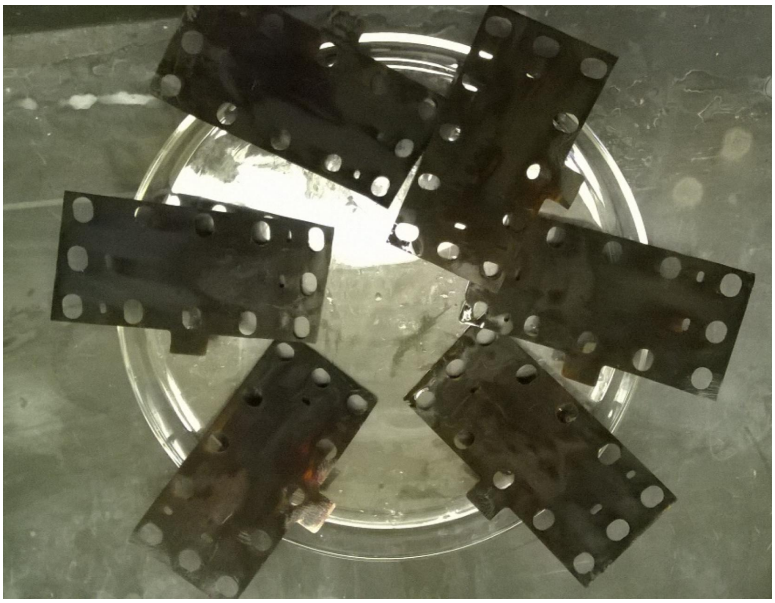

Figure 5.2. Photocathode after the first step and baking for two hours.

as electrodeposition time in the second step. Intense research has been performed in this work for different morphologies of hybrid of cuprous (Cu2O) and cupric (CuO) oxide.

5.1.3.1 Cupric (CuO)

After the first step of making photoelectrodes, cuprous is formed on the copper foil. This cuprous is formed in nanowire shape and length and thickness of these nanowires depending on the soaking time. Cuprous has been formed on copper foil in five different soaking times including 15, 35, 50 , 80 , and 120 minutes. One SEM image for each one is provided here and these are shown in figure 5.3 to figure 5.7. Not only do the length and thickness of nanowires increase with each soaking time, but by increasing the soaking time, the more dense areas of nanowires are formed. After only 15 minutes of soaking in the first step of making photoelectrodes, only a few nanowires have been formed with less than two micro meter length, as it is

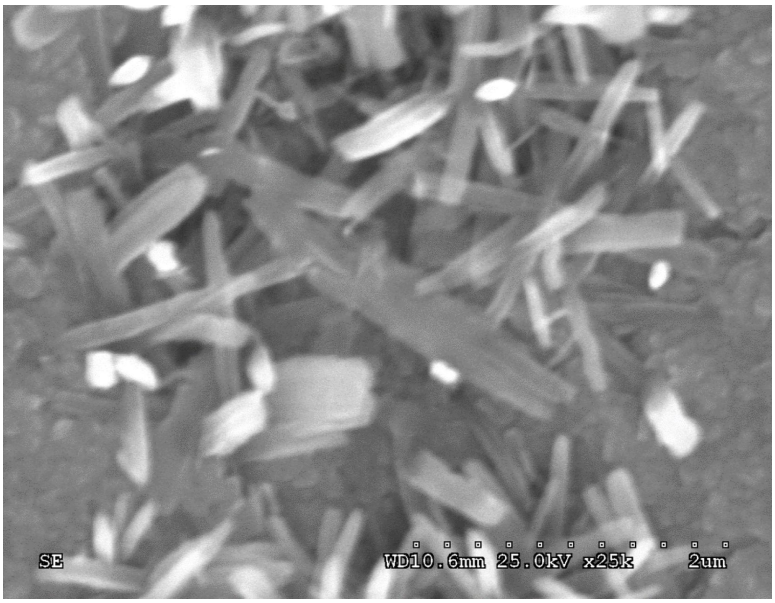

Figure 5.3. CuO nanowires after 15 minutes soaking .

shown in figure 5.3. When this time increases to 35 minutes, longer nanowires are formed up to 10 micro meters, but still there are a lot of areas on the electrodes with very small number of nanowires, as it is shown in figure 5.4. The perfect dense areas of long nanowires are formed within 50 minutes of soaking, as it is shown in figure 5.5, and whitin 80 minutes of soaking, very dense nanowires are formed. Figure 5.6 shown these nanowires. In this time curved nanowires are formed, and by increasing the soaking time to 120 minutes as it is shown in figure 5.7, the density of nanowires increases sharply and more curved nanowires are formed.

5.1.3.2 Cuprous oxide (Cu2O)

Cuprous oxide has crystal morphology and in the second step of the making of photoelectrodes, these crystals will be added onto the cuprous oxide nanowires. To confirm these crystal morphologies only the second step of making photo electrodes,electrodeposition, has been performed on pure copper foils. After 10 minutes

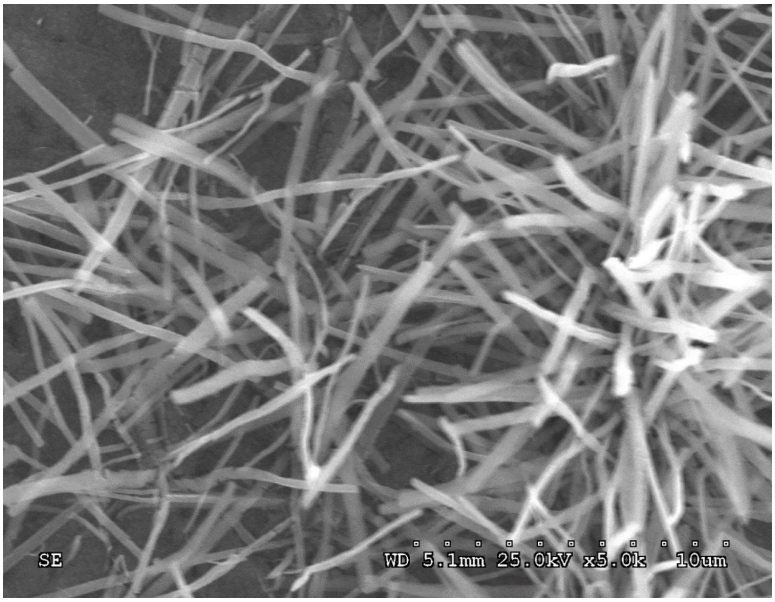

Figure 5.4. CuO nanowires after 35 minutes soaking.

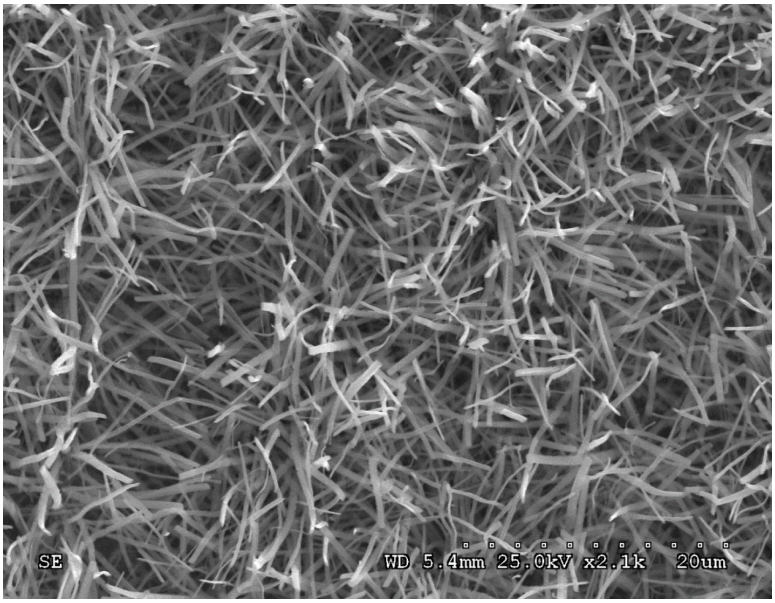

Figure 5.5. CuO nanowires after 50 minutes soaking.

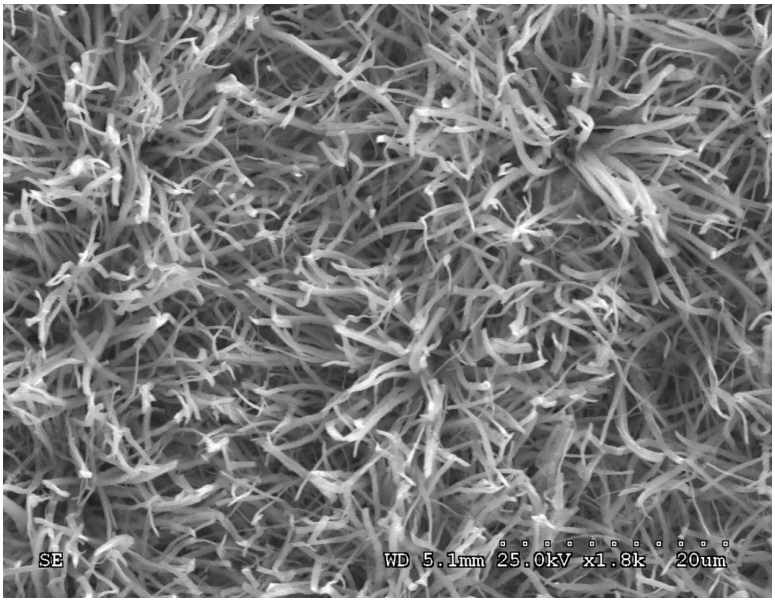

Figure 5.6. CuO nanowires after 80 minutes soaking.

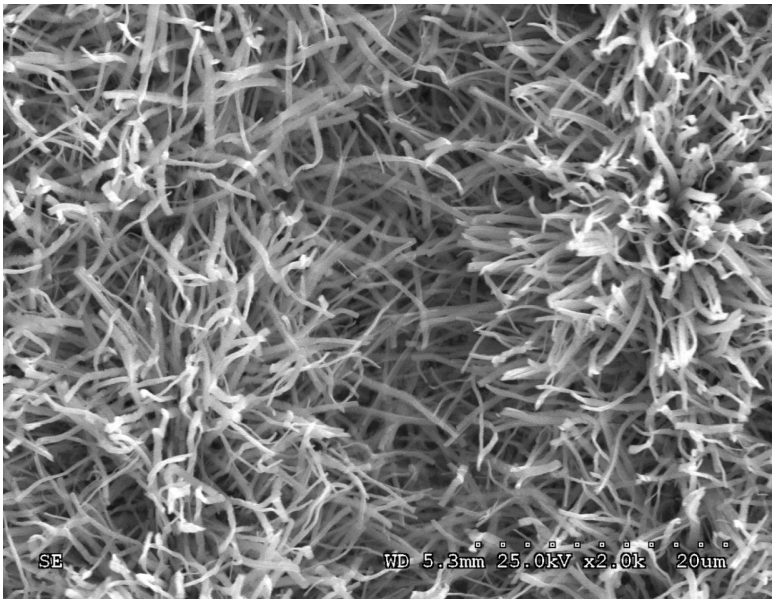

Figure 5.7. CuO nanowires after 120 minutes soaking.

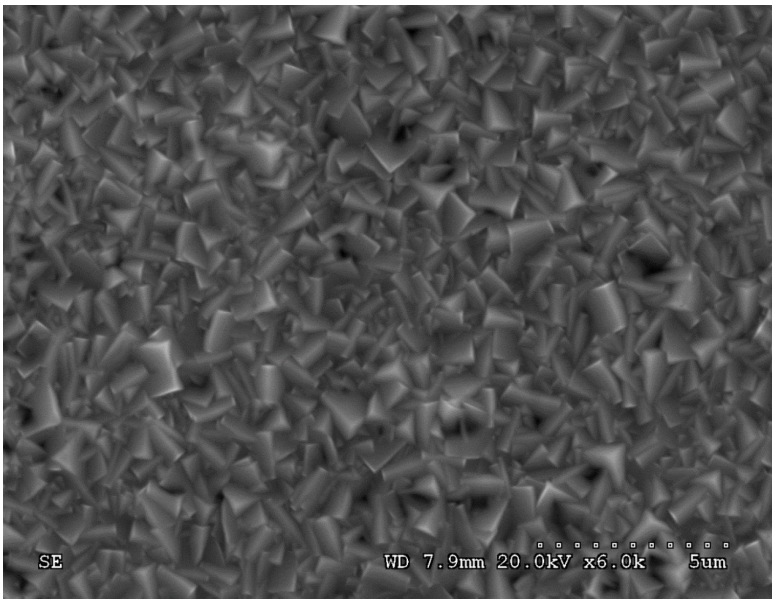

Figure 5.8. Cu2O crystals after 10 minutes electro deposition on a copper foil.

electrodeposition the crystals are formed like it is shown in figure 5.8, and after 30 minutes of electrodeposition larger crystals of cupric oxide are formed as it is shown in figure 5.9.

5.1.3.3 Hybrid of cuprous (Cu2O) and cupric (CuO) oxide

Different types of the hybrid of cuprous (Cu2O) and cupric (CuO) oxide have been made as will be mentioned later on in the results section, but to study the morphology of these hybrid, five different types of hybrid have been selected and analyzed.

5.1.3.3.1 (CuO) 15 - (Cu2O) 10 A copper foil has been soaked for 15 minutes and then baked for 2 hours in an oven for the first step to have CuO nanowires, and then crystals of Cu2O have been electrodeposited on nanowires for 10 minutes. Figure 5.10 shown this morphology. Both nanowire morphology and crystal morphology are

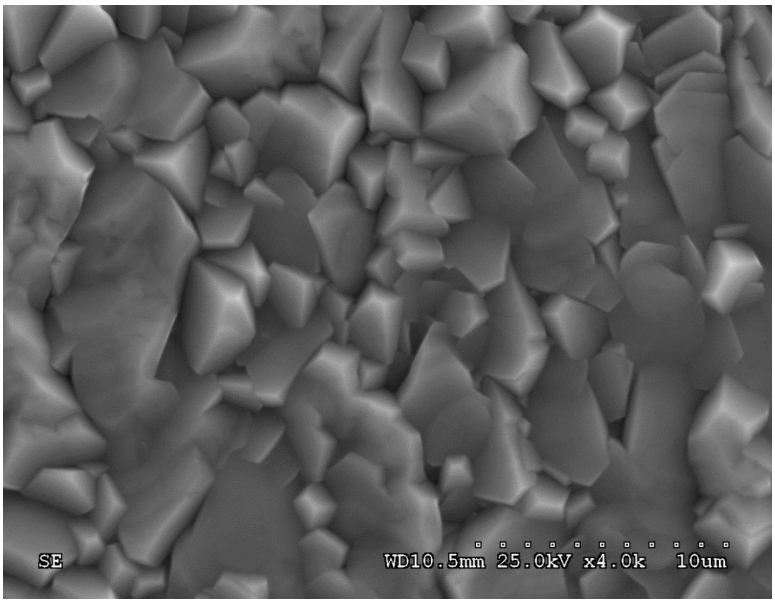

Figure 5.9. Cu2O crystals after 30 minutes electro deposition on a copper foil.

hybrid together on the surface. Because of the short time of the electrodeposition, still nanowires dominate on the surface.

A schematic illustration of CO2 photoelectroreduction on CuO/Cu2O nanorod arrays is shown in Figure 5.11c. An SEM magnification of isolated CuO nanorods decorated with Cu2O nanocrystallites is included in the figure 5.11.

5.1.3.3.2 (CuO) 50 - (Cu2O) 10 To make this hybrid,CH 50 ED 10, soaking time in the first step increased to 50 minutes; meanwhile electrodeposition time is kept to 10 minutes in the second step of the photoelectrodes making.

This sample, (CuO) 50 - (Cu2O) 10, has thicker nanowires than the first sample, (CuO) 15 - (Cu2O) 10. This morphology is shown in figure 5.12.

5.1.3.3.3 (CuO) 80 - (Cu2O) 15 To make a hybrid ready for this electrode, CH 80 ED 15, the soaking time for making nanowires of CuO increased to 80 minutes, and then crystals of Cu2O are formed by 15 minutes of electrodepositing. Increasing

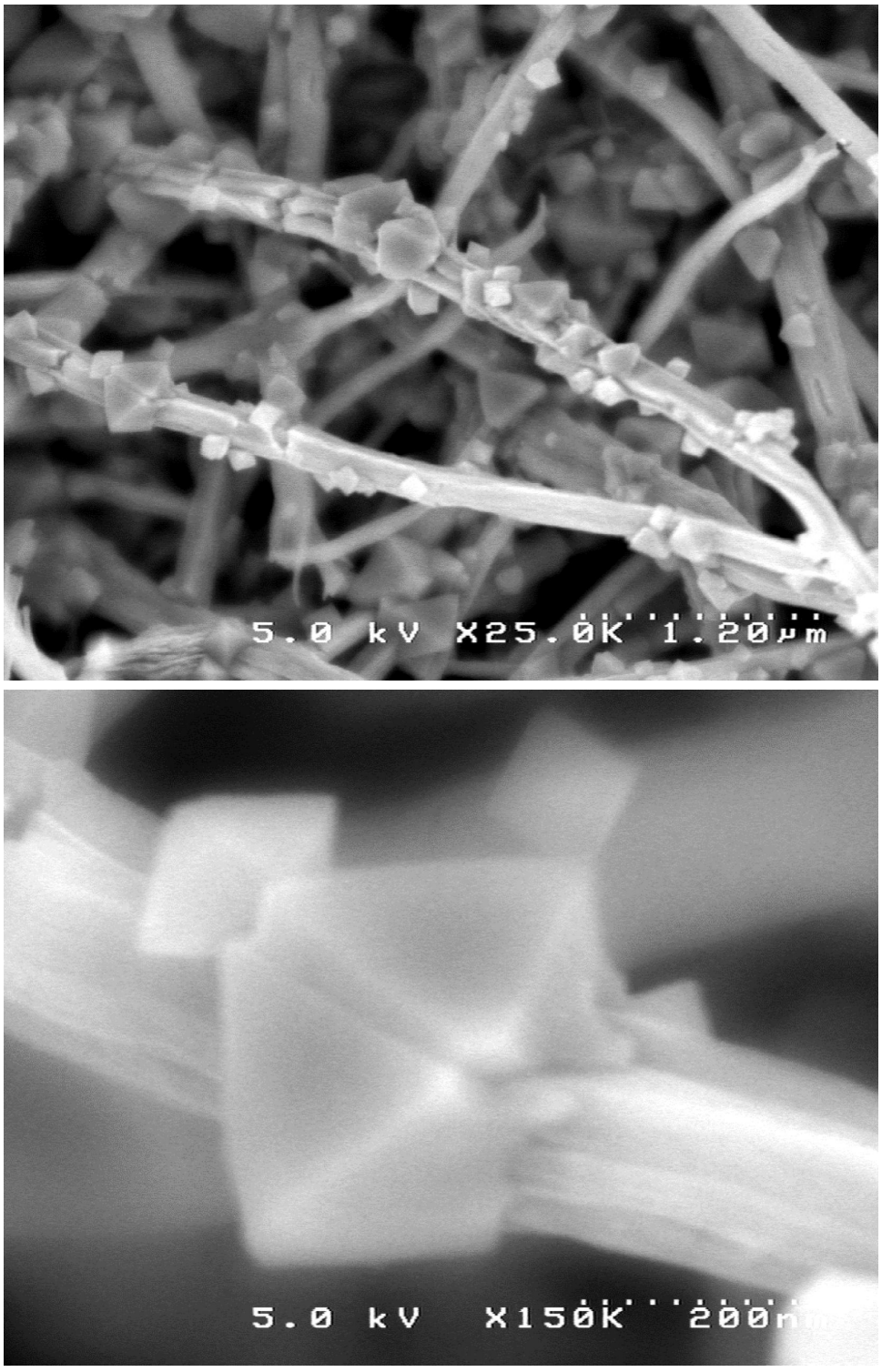

Figure 5.10. Some SEM images of hybrid of Cu2O crystals after 10 minutes electro deposition on over nanowires of CuO formed by 15 minutes soaking.

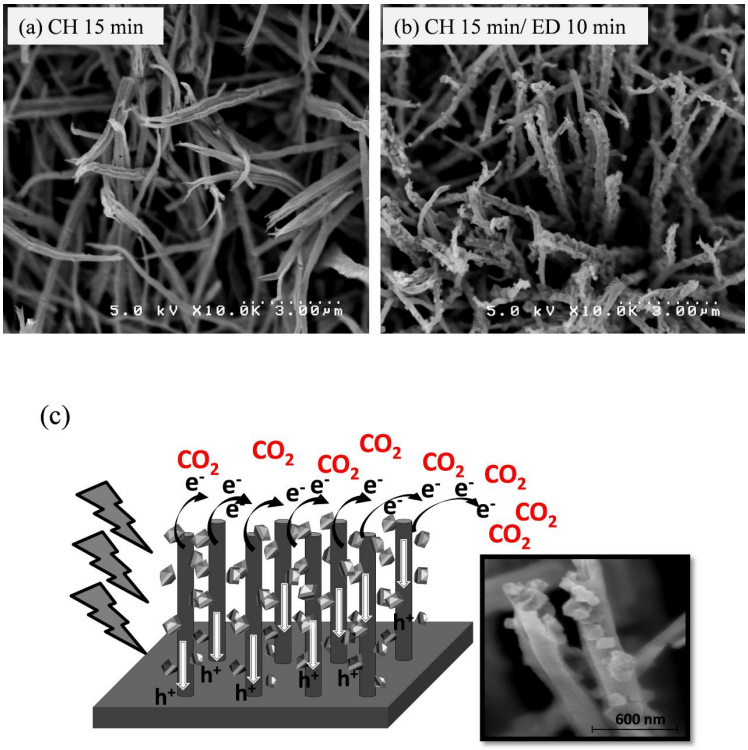

Figure 5.11. SEM images of CuO/Cu2O hybrid nanorods arrays (a) Cu chemical oxidation for 15 min before (b) and after Cu2O electrodeposited for 10 min and insert high resolution (c) a sketch of the solar photoelectrosynthesis of alcohols from carbon dioxide.

the electrodepositing time from 10 minutes to 15 minutes has an outstanding effect on the crystals formation of Cu2O. The 5 minutes extra of electrodeposition results in covering all of CuO nanowires with Cu2O crystals as it is shown on figures 5.13.

5.1.3.3.4 (CuO) 80 - (Cu2O) 20 To have a better vision of the effect of the electrodeposition time, this sample is prepared. The soaking time to form CuO nanowires is same as the last sample, but the electrodeposition time increased to 20

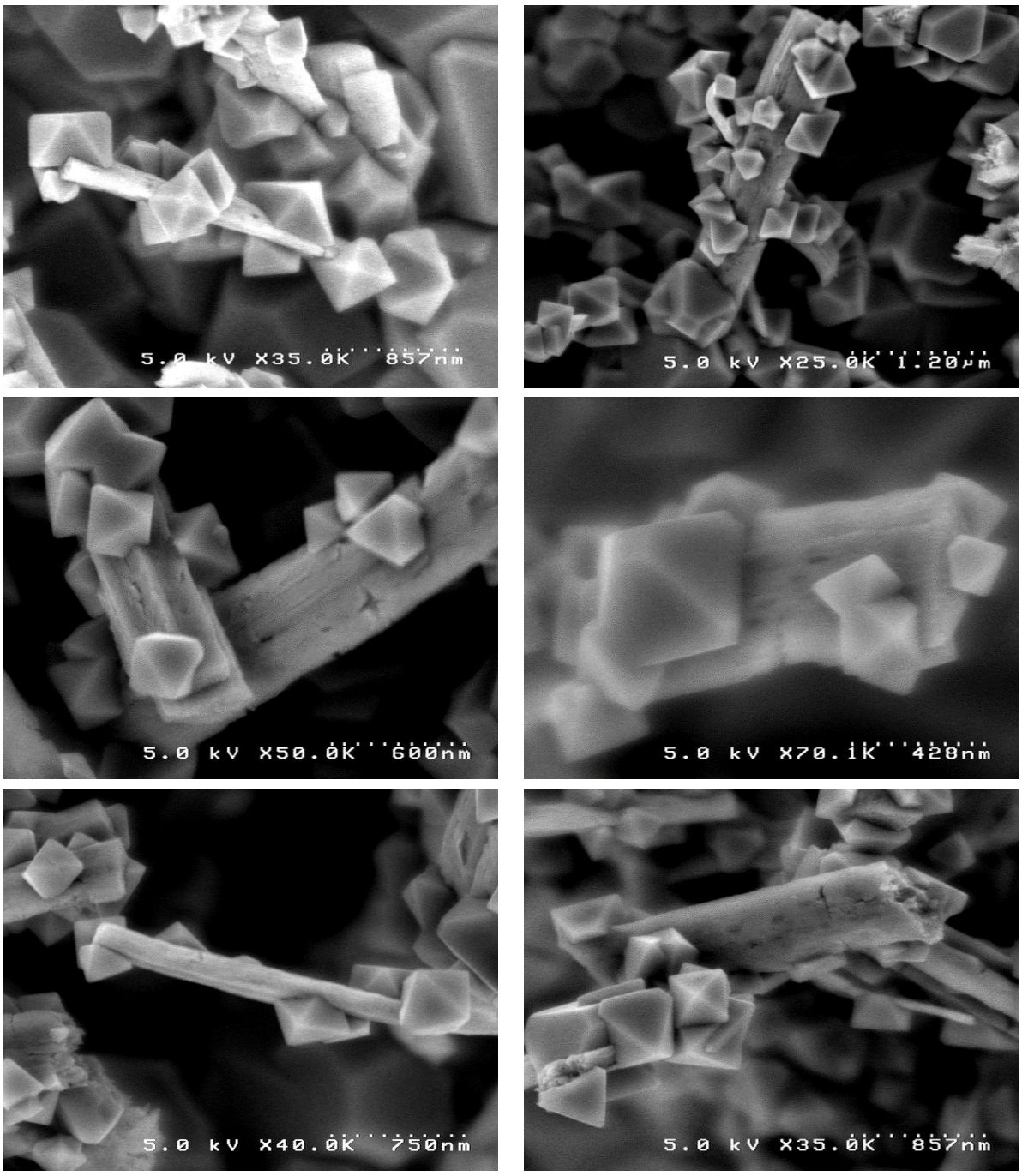

Figure 5.12. SEM images of hybrid of Cu2O crystals after 10 minutes electro deposition on over nanowires of CuO formed by 50 minutes soaking .

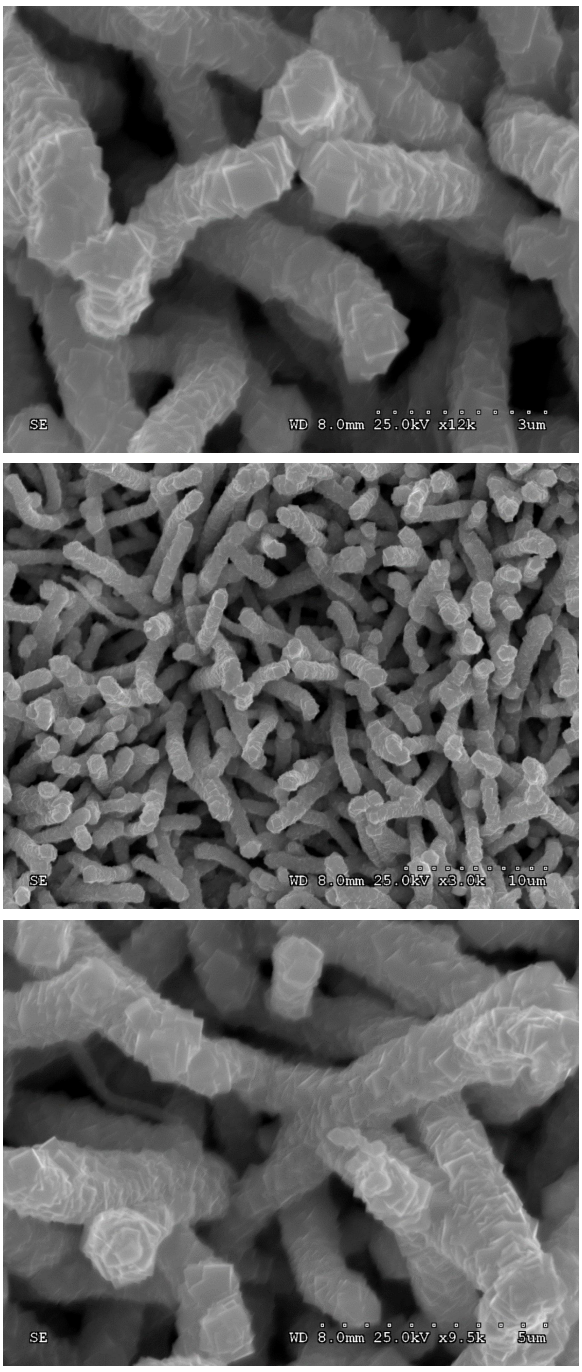

Figure 5.13. SEM images of hybrid of Cu2O crystals after 15 minutes electro deposition on over nanowires of CuO formed by 80 minutes soaking .

minutes. More crystal formation is shown on the SEM images of this sample in figure 5.14.

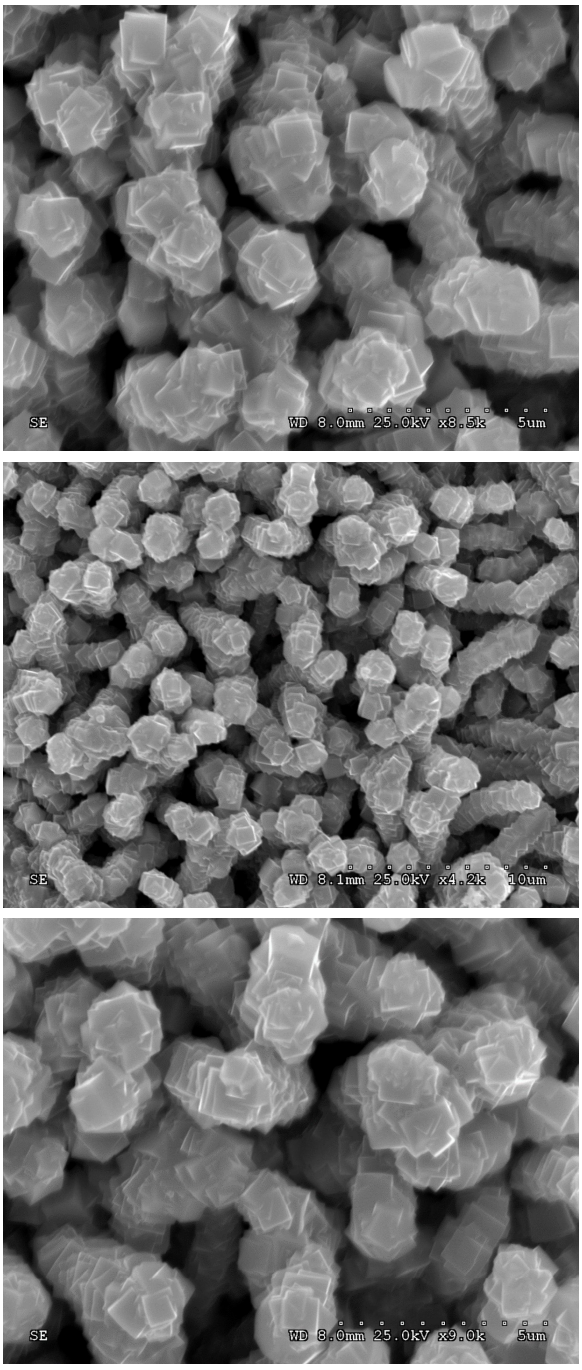

Figure 5.14. SEM images of hybrid of Cu2O crystals after 20 minutes electro deposition on over nanowires of CuO formed by 80 minutes soaking.

5.1.3.3.5 (CuO) 80 - (Cu2O) 30 If the electrodepositing time increased to 30 minutes, all CuO nanowires will be covered by Cu2O crystals. Figure 5.15 shows the surface of the photo electrode is fully covered with Cu2O crystals.

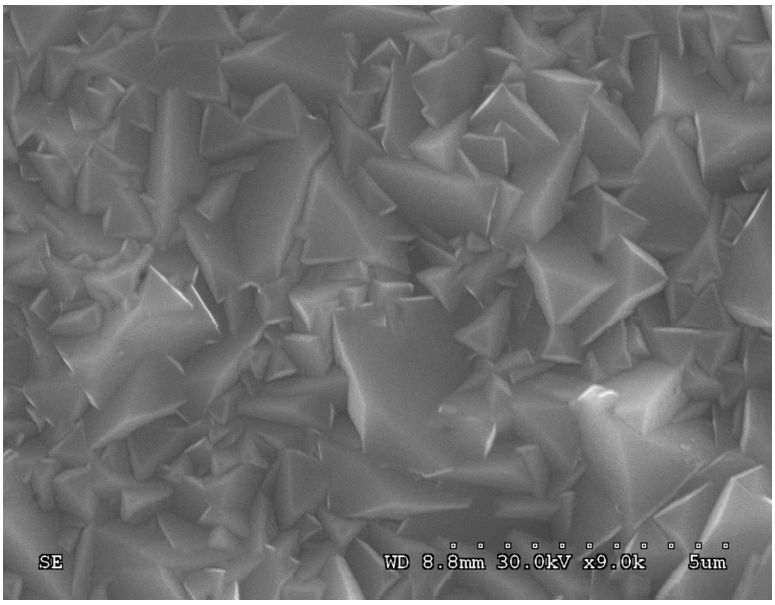

Figure 5.15. SEM image of hybrid of Cu2O crystals after 30 minutes electro deposition on over nanowires of CuO formed by 80 minutes soaking.

5.1.4 More characterization

To better understand the chemical composition of the surface of the photoelectrodes some more characterization have been done. SEM results have been presented in the last section and in this section XRD and XPS results have been reported.

5.1.4.1 XRD (X-ray diffraction measurement)

The X-ray diffraction measurement (XRD) of the (CuO) 15 - (Cu2O) 10 is shown in figure 5.16. Also XRD result for the only first, soaking for 15 minutes and baking for 2 hours, is shown in the same figure. XRD test shows after only the

first step and having nanowires of CuO the big peak of CuO appears on around 2 theta = 32 and 2 theta = 37 and there is no sign of any Cu2O. After performing the electrodeposition for 10 minutes on top of nanowires of CuO, XRD test was repeated. The result shows a peak for Cu2O around 2 theta = 34 appears and also two peaks of CuO shows less intensity at this step. It demonstrates after the first step of making photo electrodes, CuO as a chemical components formed on the surface and after the second step, electrodeposition, the hybrid of CuO and Cu2O appears on the copper foil.

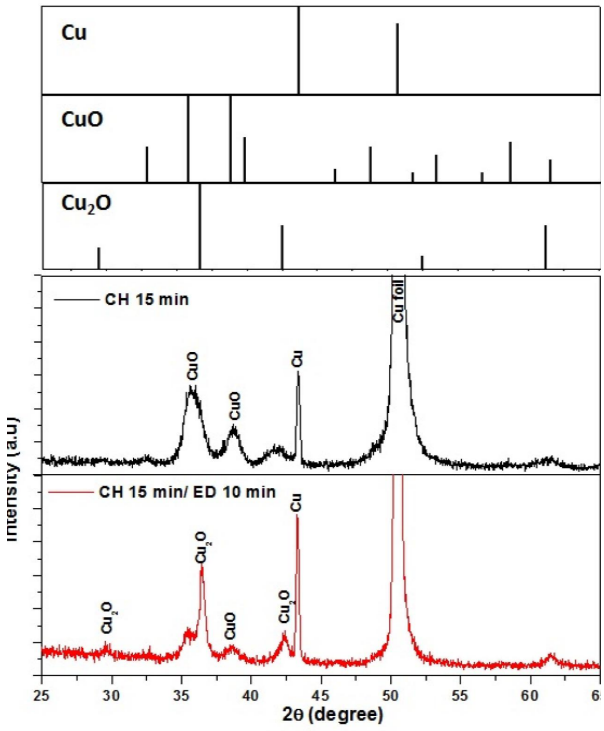

Figure 5.16. XRD results for CuO formed by 15 minutes soaking and hybrid of Cu2O crystals after 10 minutes electro deposition on over nanowires of CuO formed by 15 minutes soaking.

5.1.4.2 XPS (X-ray photoelectron spectroscopy)

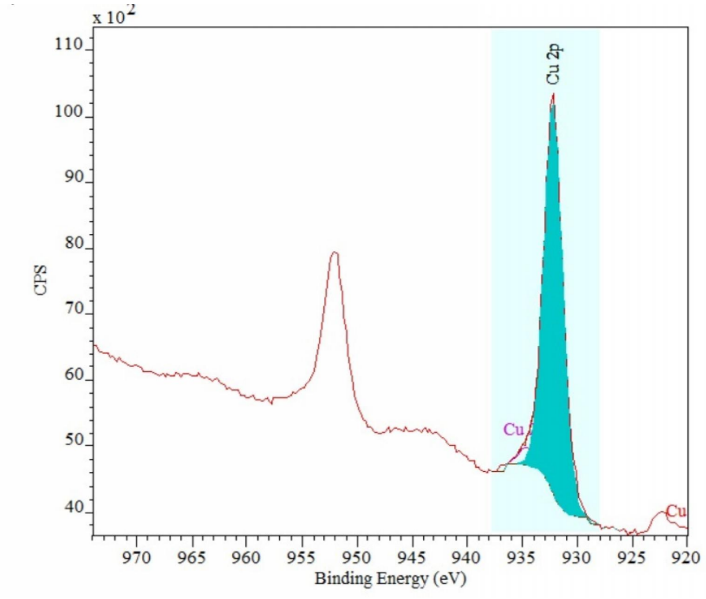

Figure 5.17. 95% of the photo electrodes, CH 50 ED 20, are covered by Cu2O.

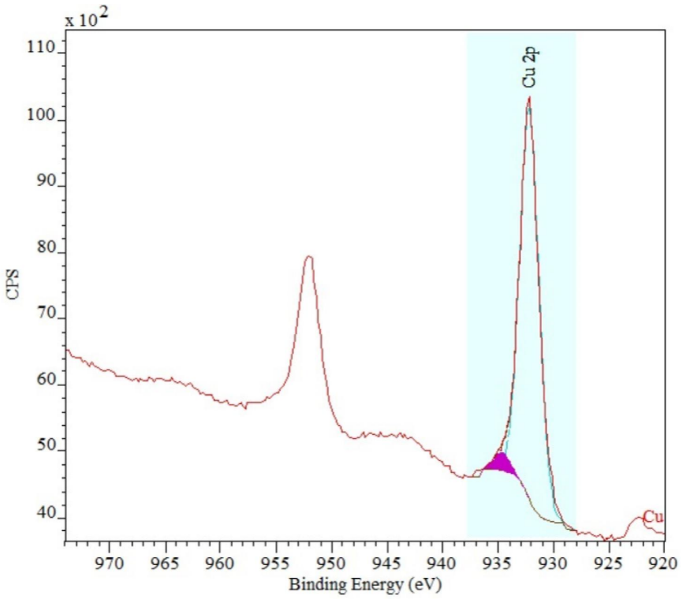

Figure 5.18. 5% of the photo electrodes, CH 50 ED 20, are covered by CuO.

The XRD test helped to qualify the chemical components of the photoelectrodes, now to quantify these two chemical composition results of X-ray photoelectron spectroscopy (XPS) test is reported. One electrode with only nanowires of CuO after 50 minutes of soaking time,CH 50, and the other photoelectrode,CH50 ED20, were made for this X-ray photoelectron spectroscopy (XRD) test. Based on this test and analyzing with CasaXPS software 95% of the electrode surface is covered by Cu2O crystals and 5% is covered by CuO nanowires. XPS results are shown in figure 5.17 and figure 5.18.

5.2 Product detection

5.2.1 Introduction

To detect the alcohols in this work, a Shimadzu gas chromatography - mass spectrometry instrument (GC-MS) was used. To protect the GC column it is necessary to take the salt out of the samples before injecting to GC-MS. For this purpose two different approaches were selected. At the beginning, resins were used to separate the salt from samples and the second approach was changing the glass liner of the GC.

5.2.2 Using Resins

For sample preparations after each test of the microfluidic reactor 2 ml of each sample was placed in 2 grams of resins and a small stir bar. The sample was stirring for around 12 hours, overnight. Then 1 ml of each sample was placed on GC-MS vial and 1 /muL of liquid was injected into the gas chromatography - mass spectrometry instrument (GC-MS). A Shimadzu GC-MS-2010SE chromatograph with a MS QP2010 detector and a AOC-4 20S sampler was used. The chromatographic column was Shimadzu SHRX105MS (30-m length and 0.25-mm inner diameter, part # 220-

94764-02), and helium was used as the carrier gas. The initial oven temperature was 45. The injection port and detector temperature were 200C. The temperature of the ion source (EI, 70eV) was 250. The MS detector was set at 250. Samples were run in SCAN mode over the mass-to-charge. To have an accurate calibration curve, different concentrations of three alcohols in same salt concentration of electrolyte were prepared and injected to the GC. GC-MS results for three concentrations are shown in figure 5.19.

(m/z) ratio range of 29-150 for determination of retention times. Detection at m/z of 31 and 45 was used for methanol and ethanol, while m/z of 59 were associated to the presence of isopropanol. The calibration curve based on the SIM mode for 5 different concentrations of Methanol, Ethanol and Isopropanol is presented in figure 5.20. As it is shown for the calibration of Methanol in case of zero area under the curve of GC result, the concentration reported by the calibration curve is not zero. This is a bad effect of the resin on the samples, because by injection of DI water, after putting on resin for 12 hours, GC-MS results show some peak for m/z 31 close to methanol. These peaks are actually related to materials in the resin like Trimethylamine. By injection of pure Trimethylamine in GC-MS similarity of the peaks of m/z 31 to m/z 31 peaks on sample results are confirmed. Because of this problem the other method is applied instead of using resins.

5.2.3 Changing the splitter glass liner

The other method used in this work for the first time is changing the glass liner in the GC splitter. After the injection port in GC the sample goes to the splitter and sample is heated up to 200 degree celsius and diluted with the career gas. This dilution depends to the split ratio on the GC software. For all of GC tests in this work split ratio was 20. It means the injected sample diluted with Helium as the

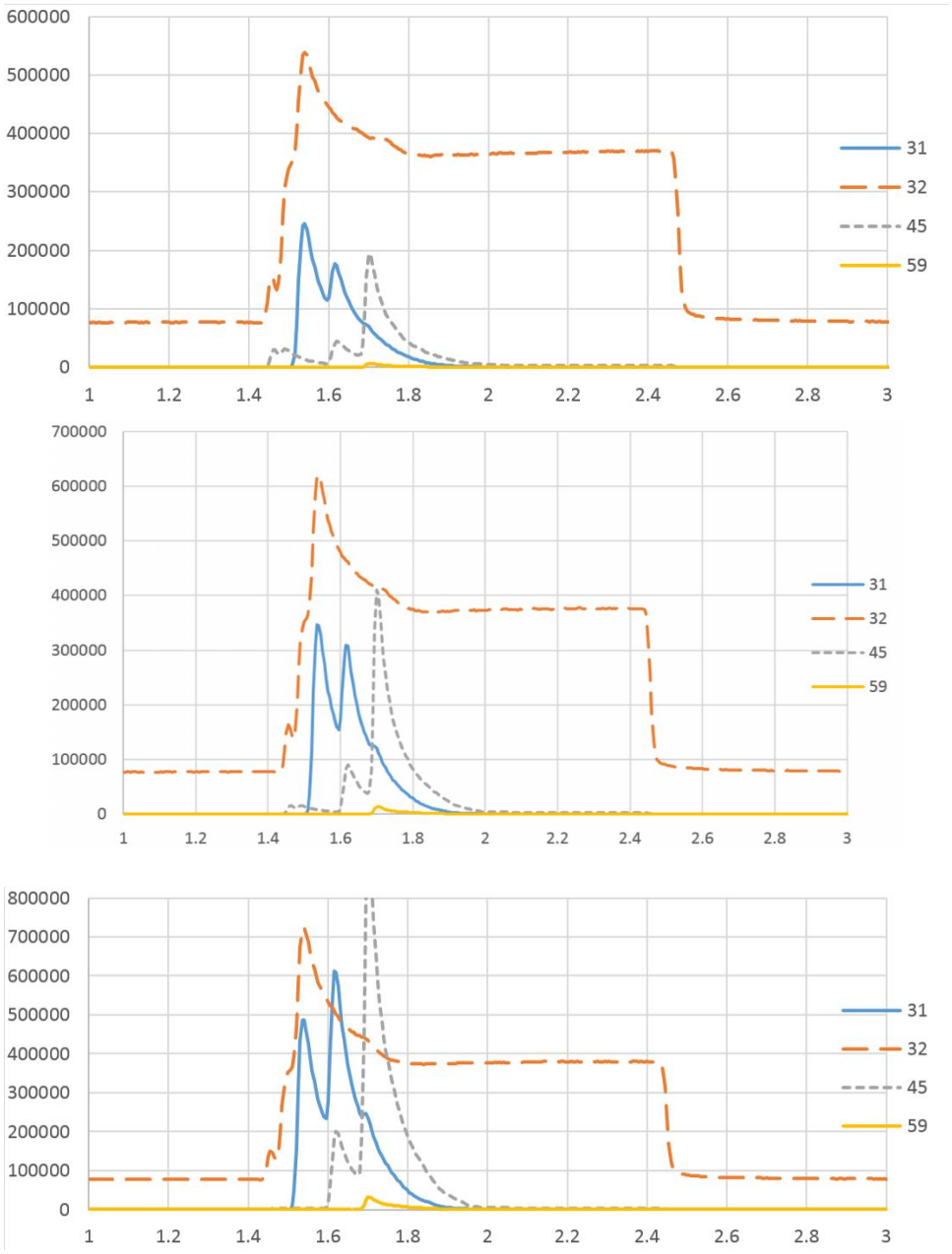

Figure 5.19. Gas chromatographymass spectrometry results for 3 different concentrations of calibration bufferss with 250/mu M, 500 /mu M, and 1250 /mu M 3-Alcohols.

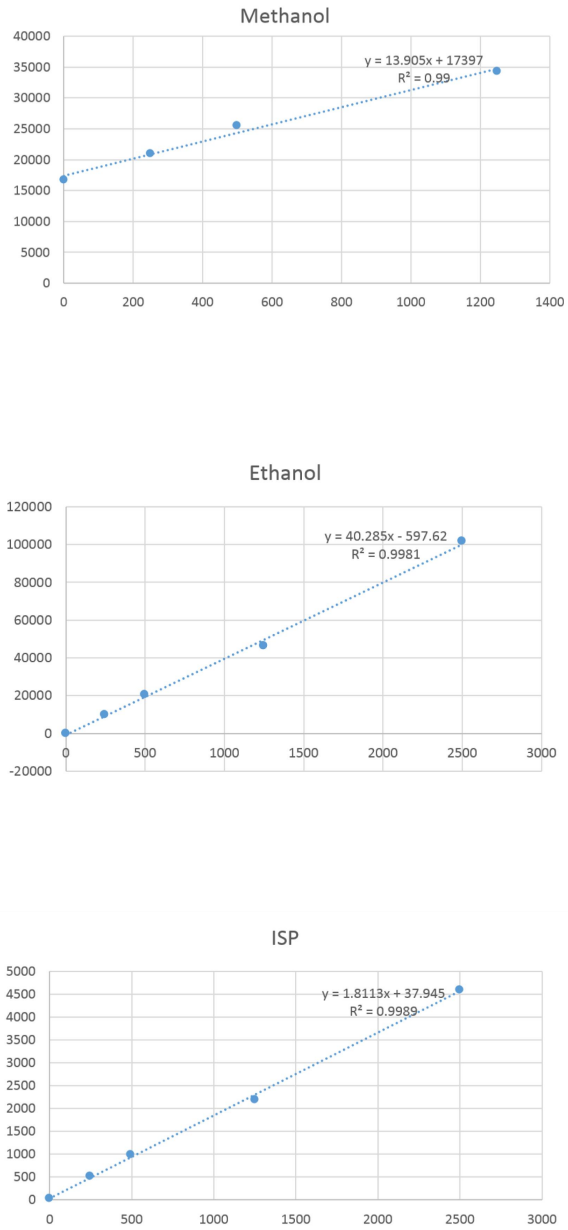

Figure 5.20. Calibration curve for 3-Alcohols.

carrier gas and only 1/21 of it goes to the column. It is obvious by this very low concentration, 0.1 M, of salt in samples, this small amount, 1 μL, of injection, and this only 5% of sample going to the column, a very small amount of salt could have gone to the column, if the glass liner did not have any filter and if it was not in high temperature. Typically, for salt less samples each glass liner is changed after 500 injections. Glass liners for this work was changed after each 50 injections to make sure no salt can go to the column. Figure 5.21 shows one of the used glass liners.

Figure 5.21. A splitter glass liner for GC-MS..

Changing the GC-MS glass liner made it possible to do GC-MS test right after testing of microfluidic reactor and not waiting for 12 hours to stir samples with resin. To make a calibration curve this time a mixture of 6 first alcohols were used and also by optimizing the temperature program peaks separation happened for these alcohols. For the four first alcohols, Methanol, Ethanol, n-Propanol, and n-Butanol (m/z) 31 was selected and for n-Pentanol and n-Hexanol (m/z) 55 was selected.

As it is shown in figure 5.22, all first four alcohols have a good separation by using a right temperature programing. Calibration curves for these samples are

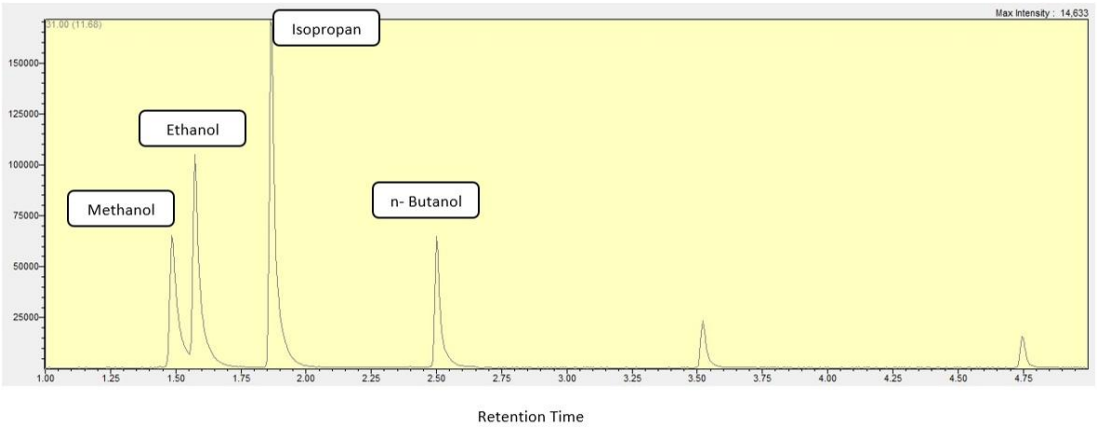

Figure 5.22. Separation of fours alcohols by GC-MS for (m/z=31) .

presented in figure 5.23. As it is shown this time all calibration curves pass the point (0, 0).

5.3 Produced alcohols

In this section some of the detected desired products are reported.

5.3.1 Photoelectroreduction of Carbon dioxide using hybrid CuO/Cu2O arrays

figure 5.22a-b contains representative photocurrent/potential (iph/V) profile under chopped AM 1.5 simulated solar illumination for CuO/Cu2O hybrid films. These profiles depicting cathodic currents are clear diagnostic of a p-type photoelectrode behavior in the potential range extending from 0.2 to -0.7 V vs Ag/AgCl. Specifically, figure 5.22a compares the photoelectrochemical performance in 0.1 M NaHCO3 saturated with carbon dioxide and N2, respectively. It is worth noticing that the photocurrent is almost double in the presence of Carbon dioxide and thus pointing out to the Carbon dioxide capability of using more photogenerated electrons from the photoelectrode than in case of the control solution in which it is just water

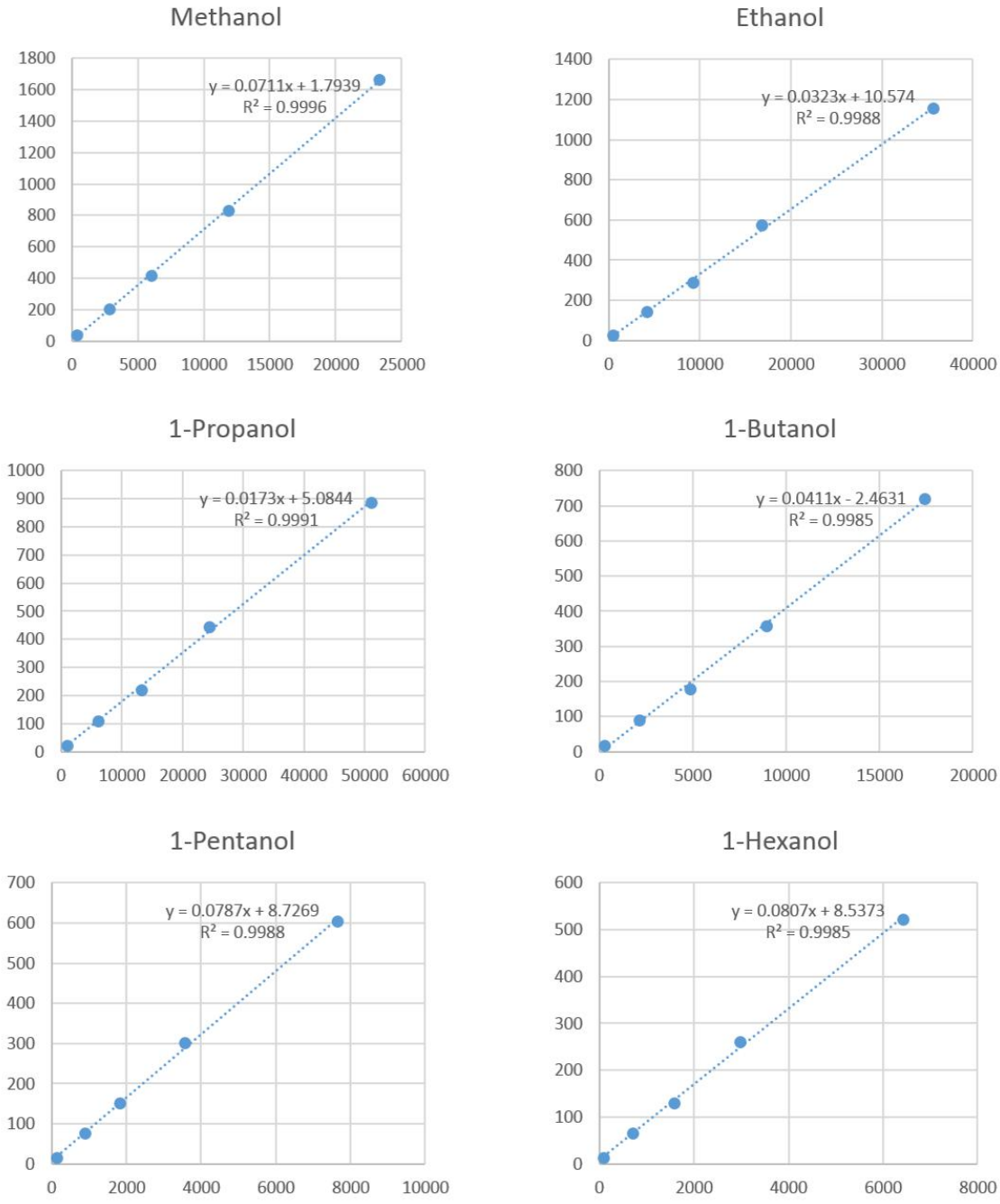

Figure 5.23. Calibration curve for 6 alcohols.

photoreduction to H2 and thus confirming that Carbon dioxide is a better electron scavenger than water.

The efficiency of this new two-step process for preparation of hybrid films is clearly shown in figure 5.24b in which three photoelectrodes are compared. The comparison of CuO/Cu2O hybrid with those of individual formation of chemical+oxidation (CH 15) and electrodeposition (ED 10) in Carbon dioxide -saturated 0.1 M NaHCO3 shows that the CuO/Cu2O hybrid performed the best for the phototoelectroreduction of Carbon dioxide and in full agreement with the band-edge alignment of both oxide phase as have reported [162, 168]. The stabilization role of electrodeposited Cu2O is clearly seen in figure 5.24b and seems to be rooted in the capability of Cu2O to adsorbed Carbon dioxide on its surface [176] . Additionally, these nanowire arrays are of higher surface area than those reported in other works [168, 162], and therefore these arrays are more effective to enhance performance by promoting the electron transport to Carbon dioxide and to reduce electronhole recombination as is schematically presented in Figure 5.11.

figure 5.24c is quite revealing of the performance of a microfluidic photoelectrochemical reactors with three channels. Comparison with a conventional photoelectrochemical cell without electrolyte flow at -0.3 V indicates that the photocurrent density vs. time profile is 5 times higher for a microfluidic photoelectrochemical reactors with three channels. The photocurrent in the a microfluidic photoelectrochemical reactors with three channels is not only much higher but also much stable over the course of 5 hours, indicating of the efficiency current depends not only on the efficiency of the photoelectrode but also on the reactor configuration and electrode assembling. In fact, to perform a photoelectrochemical process a power (or sunlight) supply is needed to make the process thermodynamically favorable, but also the overpotential effects should be taken into account and these phenomena strongly depend on the

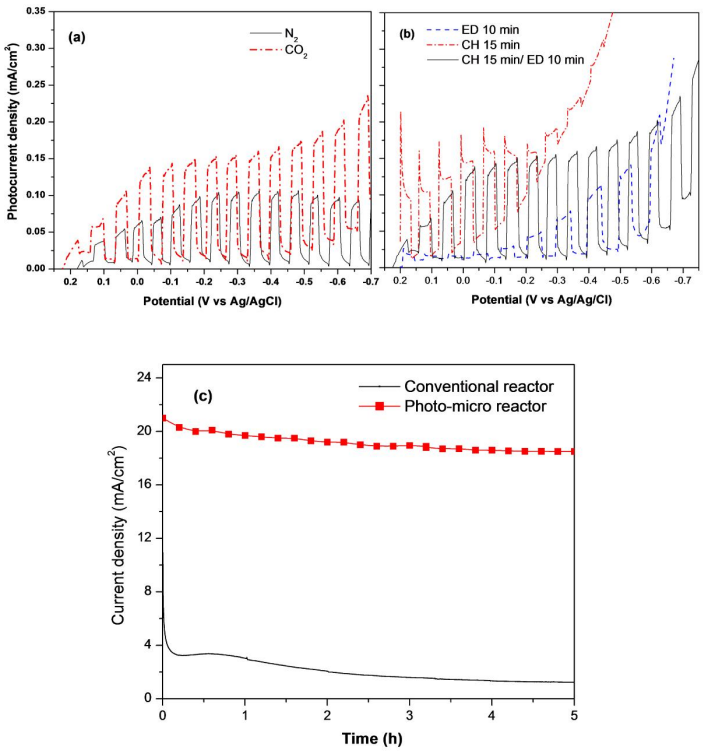

Figure 5.24. (a) Comparison of photocurrent/potential profiles for CH 15/ED 10 electrode in 0.1 M NaHCO3 in N2 and CO2 saturated solutions respectively; (b) comparison of photocurrent/potential profiles for CH 15 min, ED 10 min and CH 15/ED 10 electrode in 0.1 M NaHCO3 saturated with CO2 , and (c) photo-current density of CuO/Cu2O hybrid CH 15/ED 10 nanorods arrays in a microfluidic reactor (red trace) and conventional reactor (black trace) under same CO2 saturated 0.1 M NaHCO3 solution.

reactor design. The current density in the photo micro system was almost 5 times higher than conventional because when current is flowing in an electrochemical cell, there is a potential drop between the reference electrode and the working electrode. This voltage drop is caused by the distance between the two electrodes. On the a microfluidic photoelectrochemical reactors with three channels this distance is de-

creased down to about 100 micrometer but in a conventional cell this distance is about a few centimeters. This decrease in distance promotes a significant increase of the photocurrent magnitude.

5.3.2 Enhanced product formation in a microfluidic photoelectrochemical reactors

In relation to the products formed during photoelectrolysis, figure 5.25 presents a bar diagram of the liquid products (alcohols) formed during irradiation of CuO/Cu2O hybrid CH 15/ED 10 nanorods arrays at -0.3 V vs Ag/AgCl in the microfluidic photoelectrochemical reactors with three channels containing 0.1 M NaHCO3- CO2 saturated as electrolyte. GC-MS test for these results have been done with putting samples on resins. Very importantly, three main alcohols were formed: methanol, ethanol and isopropanol. Besides, the higher photocurrent in the microfluidic photoelectrochemical reactors with three channels (figure 5.25) nicely agrees with the higher amount of photogenerated products that are totaling 5-6 times higher than in the conventional cell.

Interestingly, the product distribution was found to change as a function of the irradiation time. In fact, methanol, ethanol and Isopropanol were formed in initial two hours but after approximately 3 hours of irradiation higher carbon chain products were found. The possible explanation of shift product distribution away from methanol toward longer chain hydrocarbons is that probably the formation of C-C bonds is the rate determining step of the whole carbon dioxide reduction process, but more specific investigations are needed to confirm this hypothesis. It is worth to notice that the total product remains almost as constant, indicating some deactivation of the photoelectrode likely related to Cu2O photocorrosion[168, 162].

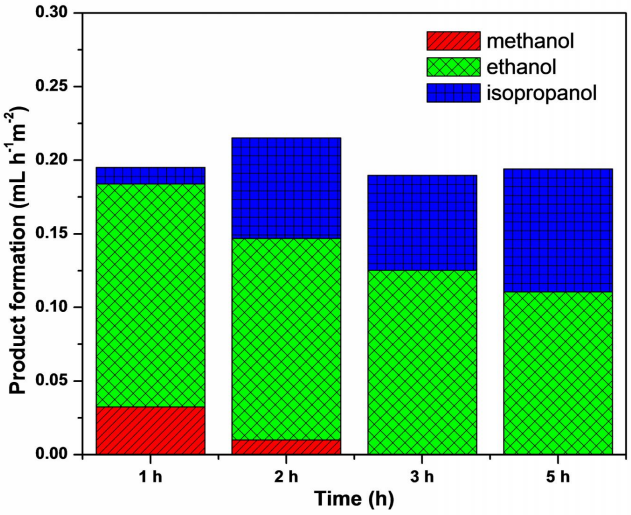

Figure 5.25. Product distribution as a function of irradiation time for irradiated CuO/Cu2O hybrid CH 15/ED 10 nanorods arrays at -0.3 V in a FPECR containing 0.1 M NaHCO3 aqueous solution saturated with CO2.

5.3.2.1 Optimization of hybrid of CuO and Cu2O to enhanced product formation in a microfluidic photoelectrochemical reactors

In this section, comprehensive results have been reported to select the best photocathode for microfluidic photoelectrochemical reactors. For this purpose, about 30 different types of hybrid of Cu2O and CuO were prepared and photocurrent of each in Carbon dioxide-saturated 0.1M Na2SO4 aqueous solution was measured to see which photocathode releases more photocurrent under solar simulator with -0.6 V vs Ag/AgCl, as results are shown in table 5.1. Based on this comprehensive study, the photocathode with 80 minutes of soaking time and 20 minutes, CO80/ED20, was selected as the best photocathode to use in microfluidic photoelectrochemical reactors. This photocathode was selected because of high photocurrent density, 0.91 mA/cm2, and also having a hybrid of both Cu2O and CuO. As it was mentioned on the first section of this chapter, when the electrodepositing time passes 20 minutes all

surfaces of CuO nanowires will be covered by Cu2O. For this reason although there are some other photocathodes with a little bit more current density, this CO80/ED20, has been selected.

Table 5.1. CuO/Cu2O photoelectrodes prepared by two-step strategy (CO and ED) along with photocurrent in CO2-saturated 0.1M Na2SO4 aqueous solution

Photoelectrode name	1st step (CO)	2nd step (ED)	Iph -0.6 V
CO15/ED5	15 min	5 min	0.10
CO15/ED10	”	10 min	0.14
CO15/ED20	”	20 min	0.09
CO15/ED30	”	30 min	0.17
CO35/ED5	35 min	5 min	0.10
CO35/ED10	”	10 min	0.20
CO35/ED30	”	30 min	0.18
CO35/ED45	”	45 min	0.14
CO50/ED5	50 min	5 min	0.45
CO50/ED10	”	10 min	0.36
CO50/ED20	”	20 min	0.20
CO50/ED30	”	30 min	0.43
CO80	80 min	N/A	0.5
CO80/ED10	”	10 min	0.54
CO80/ED15	”	15 min	0.71
CO80/ED20	”	20 min	0.91
CO80/ED30	”	30 min	1.14
CO80/ED45	”	45 min	1
CO80/ED60	”	60 min	0.25
CO120	120 min	N/A	0.75
CO120/ED10	”	10 min	0.84
CO120/ED20	”	20 min	0.68
CO120/ED45	”	45 min	1.11
CO120/ED60	”	60 min	0.74
ED 30	N/A	30 min	
ED 45	N/A	45 min	0.73

5.3.2.2 The optimized hybrid to enhanced product formation in a microfluidic electrochemical reactors for reduction of carbon dioxide in dark

To find the best cathode to reduce Carbon dioxide a same comprehensive study were conducted for three different potentials- 0.6 , -0.8, and -1 V vs Ag/AgCl. Results are presented in table 5.2.

Table 5.2. Summary of total geometric current densities at various potential on-CuO/Cu2O electrodes. Data was observed from cyclic voltammetry in CO2-saturated 0.1M Na2SO4 aqueous

Electrode name	1st step (CO) Chemical oxidation	2nd step (Cu2O) electrodeposition (ED)	Iph -0.6 V	Iph -0.8 V	Iph -1.0 V
CO15/ED5	15 min	5 min	0	1.90	4.76
CO15/ED10	”	10 min	0	1.27	4.44
CO15/ED20	”	20 min	0	0.63	3.81
CO15/ED30	”	30 min	0	0.79	3.65
CO35/ED5	35 min	5 min	0	2.22	5.40
CO35/ED10	”	10 min	0.63	2.50	5.00
CO35/ED30	”	30 min	2.22	5.08	8.25
CO35/ED45	”	45 min	1.59	4.44	6.98
CO50	50 min	N/A	0.79	2.86	5.40
CO50/ED5	”	5 min	0.32	1.27	4.44
CO50/ED10	”	10 min	3.81	7.30	11.11
CO50/ED20	”	20 min	2.86	6.03	9.21
CO50/ED30	”	30 min	1.90	4.13	7.30
CO80/ED10	80 min	10 min	2.86	6.03	9.52
CO80/ED15	”	15 min	0.32	0.63	2.22
CO80/ED30	”	30 min	0.32	1.59	3.17
CO80/ED45	”	45 min	0	0.32	0.95
CO80/ED60	”	60 min	0.32	1.27	2.22
CO120/ED10	120 min	10 min	2.22	4.76	7.30
CO120/ED20	”	20 min	1.90	4.13	6.03
CO120/ED45	”	45 min	0	0.48	0.95
CO120/ED60	”	60 min	0.95	2.22	4.13
ED60	”	60 min	1.59	3.81	6.35
Cu foil	N/A	N/A	0	0	0.32

As it is reported on this table the maximum released current density is for an electrode with 50 minutes of soaking time and 10 minutes, CO50/ED10. Based on this results this electrode was selected for reduction of Carbon dioxide without any light.

5.3.2.3 Photocathode CH 80/ED 20

As it was shown in last section a photocathode with 80 minutes of soaking time and 20 minutes, CO80/ED20, has the best current density. This photocathode was placed in a microfluidic photoelectrochemical reactor with two channels. This reactor was tested for 6 hours under solar simulator and by applying 0.3 V vs Ag/AgCl between the reference and the working electrode. To check the products the GC-MC method with replacing a splitter glass liner was used. The average results are presented in table 5.3. These results show the current density decreases over the time and the best current density is measured on the first hour. Also the best Faradic efficiency for Isopropanol is also reported for the first hour and concentration of isopropanol decreases over the time as well as concentration of the Ethanol. The most important achievement here is having the most products in a form of isopropanol, with three carbon, instead of Methanol only with one carbon. Using a new splitter glass liner, instead of putting samples on resins, was helpful to detect produced isopropanol.

An Isopropanol peak and an Ethanol peak of (m/z = 31) in GC-MC result after 1hour test of a microfluidic photoelectrochemical reactor with two channels are presented in figure 5.26.

5.3.2.4 Cathode CH 50/ED 20 (Reduction in dark)

As it was illustrated in last section a cathode with 50 minutes of soaking time and 20 minutes, CO50/ED20, has the best current density for reduction of Carbon

Table 5.3. Result of 6 hours test of a microfluidic photoelectrochemical reactor with two channels by applying 0.3 V vs Ag/AgCl

Hour	EtOH μM	IPA μM	Current Density	EtOH FE%	IPA FE%	Total FE%
1	12.54	516.78	5.5	0.73	45.33	46.07
2	12.15	294.41	5.3	0.74	26.80	27.54
3	12.01	138.17	2.2	1.16	30.30	31.46
4	12.8	39.04	1.68	1.67	11.21	12.88
5	12	24.8	1.7	1.49	7.04	8.53
6	12	10.71	1.42	1.79	3.64	5.43

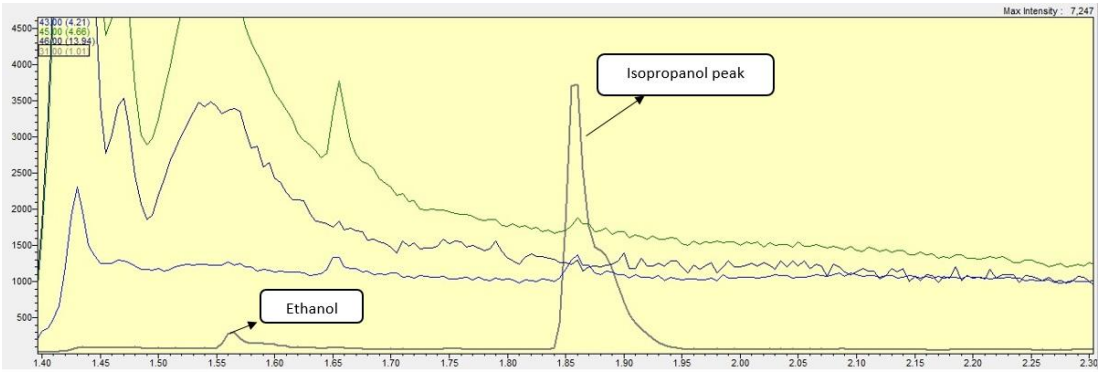

Figure 5.26. Detected Isopropanol and Ethanol in samples with GC-MS for (m/z = 31).

dioxide in dark. Microfluidic electrochemical reactors with two channels were fabricated with this electrode, CO50/ED20, as the working electrode to reduce carbon dioxide. This reactor was tested for 6 hours under by applying 1 V vs Ag/AgCl between the reference and the working electrode. To check the products the GC-MC method with replacing a splitter glass liner was used. The average results are presented in table 5.4. The same trend of decrease in current density by time was observed and also decrease in products by time. Although the appalling voltage is more than three time higher than voltage applied in microfluidic photoelectrochem-

ical reactors to reduce carbon dioxide under solar simulator, the measured alcohols products are around 30% of photo elect reduction.

Table 5.4. Result of 6 hours test of a microfluidic Electrochemical reactor with two channels by applying 1 V vs Ag/AgCl to reduce Carbon dioxide in dark

Hour	EtOH μM	IPA μM	Current Density	EtOH FE%	IPA FE%	Total FE%
1	16.09	118.6	5.1	1.01	11.22	12.23
2	20	19	4.9	1.31	1.87	3.18
3	19.4	12.7	4.1	1.52	1.49	3.02
4	15	7.8	3.5	1.38	1.08	2.45
5	14.35	8.5	2.9	1.59	1.41	3.01
6	0	7.07	2.5	1.54	1.36	2.01

5.4 Conclusion and Summary

The development and application of microfluidic photoelectrochemical reactors to produce alcohols from Carbon dioxide was demonstrated. It was furthermore showed that the hybrid CuO/Cu2O nanorod arrays prepared by a two-step process could be properly fitted in the new designed microfluidic photoelectrochemical reactors. The performance of the photoelectrode in these reactors was compared to a conventional two-compartment photoelectrochemical cell (batch system). The yield of new designed reactors were 6 times higher than batch reactor, although shows longer chains of products up to C2-C3 (ethanol and isopropanol) was found in this study. Therefore a study on the formation intermediates of C-C reaction could further improve the understanding of the mechanism which is probably quite different in batch system. The possibility to develop a photo electrochemical device able to convert Carbon dioxide to fuel and industrial chemicals would be a significant step

toward a more sustainable future.

The high surface-to-volume ratio resulting from the narrow reaction volumes in new designed reactors was shown to significantly enhance current density and faradaic efficiency. Accordingly, much higher amount of products was obtained thus demonstrating the importance of reactors for increasing product yields, improving energy efficiency, as well as controlling activity and selectivity of the photoelectrodes. All the mentioned improvement will lead to reduce capital costs.

REFERENCES

[1] D. Hoadley and M. Shell. Carbon Dioxide Information Analysis Center CDIAC . [Online]. Available: cdiac.ornl.gov

[2] (2014) The outlook for energy 2040, ExxonMobile.

[3] (2014) Nca2014. [Online]. Available: nca2014.globalchange.gov/

[4] V. Burkett, "Global climate change implications for coastal and offshore oil and gas development," *Energy Policy*, vol. 39, no. 12, pp. 7719–7725, 2011.

[5] W. N. with Paul Sztorc. (2013) Dice 2013r:introduction and users manual, second edition.

[6] [Online]. Available: http://chem-guide.blogspot.com/

[7] [Online]. Available: http://www.sparknotes.com/

[8] [Online]. Available: http://en.wikipedia.org/wiki/File:Solidoxidefuelcell.svg

[9] S. Trasatti, "Work function, electronegativity, and electrochemical behaviour of metals: Iii. electrolytic hydrogen evolution in acid solutions," *Journal of Electroanalytical Chemistry and Interfacial Electrochemistry*, vol. 39, no. 1, pp. 163–184, 1972.

[10] ——, "Electrocatalysis in the anodic evolution of oxygen and chlorine," *Electrochimica Acta*, vol. 29, no. 11, pp. 1503–1512, 1984.

[11] [Online]. Available: http://chemwiki.ucdavis.edu/

[12] W. Vielstich, A. Lamm, and H. A. Gasteiger, *Handbook of Fuel Cells: Fundamentals Technology and Applications. Vol. 1, Fundamentals and Survey of Systems*. Wiley, 2003.

[13] M. A. Russell S. Vose, Scott Applequist. Monitoring and understanding changes in extremes extratropical storms, winds, and waves.

[14] (2013) Part 9. climate of the contiguous united states. noaa technical report nesdis. [Online]. Available: http://www.nesdis.noaa.gov/technicalreports/

[15] P. A. S. Peterson, T. C. and S. Herring, "Explaining extreme events of 2011 from a climate perspective." *Bulletin of the American Meteorological Society*, vol. 93, pp. 1041–1067, 2012.

[16] (2014) Climate Change Impacts in the United States CHAPTER 4 ENERGY SUPPLY AND USE.

[17] (2014) Climate Change Impacts in the United States CHAPTER 24 OCEANS AND MARINE RESOURCES.

[18] C. Deser, A. S. Phillips, and M. A. Alexander, "Twentieth century tropical sea surface temperature trends revisited," *Geophysical Research Letters*, vol. 37, no. 10, 2010.

[19] T. M. Smith, R. W. Reynolds, T. C. Peterson, and J. Lawrimore, "Improvements to noaa's historical merged land-ocean surface temperature analysis (1880-2006)," *Journal of Climate*, vol. 21, no. 10, pp. 2283–2296, 2008.

[20] T. C. Peterson, P. A. Stott, and S. Herring, "Explaining extreme events of 2011 from a climate perspective," *Bulletin of the American Meteorological Society*, vol. 93, no. 7, pp. 1041–1067, 2012.

[21] K. Averyt, J. Macknick, J. Rogers, N. Madden, J. Fisher, J. Meldrum, and R. Newmark, "Water use for electricity in the united states: an analysis of reported and calculated water use information for 2008," *Environmental Research Letters*, vol. 8, no. 1, p. 015001, 2013.

[22] (2013) Water Quality Standards for Surface Waters. [Online]. Available: http://water.epa.gov/scitech/swguidance/standards/

[23] K. Strzepek, G. Yohe, J. Neumann, and B. Boehlert, "Characterizing changes in drought risk for the united states from climate change," *Environmental Research Letters*, vol. 5, no. 4, p. 044012, 2010.

[24] N. Furuya and K. Matsui, "Electroreduction of carbon dioxide on gas-diffusion electrodes modified by metal phthalocyanines," *Journal of electroanalytical chemistry and interfacial electrochemistry*, vol. 271, no. 1, pp. 181–191, 1989.

[25] Y. B. Vassiliev, V. Bagotsky, N. Osetrova, O. Khazova, and N. Mayorova, "Electroreduction of carbon dioxide: Part i. the mechanism and kinetics of electroreduction of co2 in aqueous solutions on metals with high and moderate hydrogen overvoltages," *Journal of Electroanalytical Chemistry and Interfacial Electrochemistry*, vol. 189, no. 2, pp. 271–294, 1985.

[26] M. Mahmood, D. Masheder, and C. Harty, "Use of gas-diffusion electrodes for high-rate electrochemical reduction of carbon dioxide. i. reduction at lead, indium-and tin-impregnated electrodes," *Journal of applied electrochemistry*, vol. 17, no. 6, pp. 1159–1170, 1987.

[27] R. Chaplin and A. Wragg, "Effects of process conditions and electrode material on reaction pathways for carbon dioxide electroreduction with particular reference to formate formation," *Journal of Applied Electrochemistry*, vol. 33, no. 12, pp. 1107–1123, 2003.

[28] M. Jitaru, "Electrochemical carbon dioxide reduction-fundamental and applied topics," *Journal of the University of chemical Technology and Metallurgy*, vol. 42, no. 4, pp. 333–344, 2007.

[29] G. Morozov, *Problems of Cosmic Biology*, 1977, ch. Theoretical Foundations of Design of Life-Supporting Systems, p. 88(in Russian).

[30] M. J. Bennett E., Eggins B. and M. E., in *Anal. Proc.*, vol. 17, 1980, p. 356.

[31] N. Z. Bockris J.O'M., *Electrochemistry for Ecologists*. Plenum Press, 1974.

[32] H. E. Kaiser U., *Phys. Chem*, vol. 77, p. 818, 1976.

[33] B. M. Tyssee D.A., Wagenknecht J.H. and C. J.L., "Some cathodic organic stntluzses involvix cabbon dioxide," *Tetrahedron Letters*, no. 47, pp. 4809–4812, 1972.

[34] N. L. GressinJ.C., Michelet D. and S. J.M., *Chim*, p. 545, 1979.

[35] J. Fischer, T. Lehmann, and E. Heitz, "The production of oxalic acid from co2 and h2o," *Journal of Applied Electrochemistry*, vol. 11, no. 6, pp. 743–750, 1981.

[36] M. Stemberg, Patent US 3 959 094, 05 25, 1976.

[37] B. M. and V. Dang, *Ertew Convers*, vol. 17, no. 97, p. 133, 1977.

[38] S. S. Russel P., Kovac N. and S. M., *J Electrochem Sot*, vol. 124, no. 9, p. 1329, 1977.

[39] J. O. Bockris, *Energy: The solar-hydrogen alternative.* Austraha and New Zealand Book Company, 1975.

[40] Y. H. Tomkiewicz M., Haynes R. and H. Y., "Environmental aspects of electrochemistry and photoelectrochemistry," in *ECS Proceedings*, vol. 18, May 1993.

[41] H. Y., "Electrochemical co2 reduction on metal electrodes," in *Modern aspects of electrochemistry.* Springer, 2008, pp. 89–189.

[42] Y. Hori, H. Wakebe, T. Tsukamoto, and O. Koga, "Electrocatalytic process of co selectivity in electrochemical reduction of co2at metal electrodes in aqueous media," *Electrochimica Acta*, vol. 39, no. 11, pp. 1833–1839, 1994.

[43] M. T. Ito K. and I. S., *Bull. Nagoya Inst. Techn*, vol. 27, p. 209, 1975.

[44] Y. Hori, K. Kikuchi, and S. Suzuki, "Production of co and ch4 in electrochemical reduction of co2 at metal electrodes in aqueous hydrogencarbonate solution," *Chemistry Letters*, no. 11, pp. 1695–1698, 1985.

[45] H. Noda, S. IDEKA, Y. Oda, K. Imai, M. Maeda, and K. Ito, "Electrochemical reduction of carbon dioxide at various metal electodes in aqueous potassium

hydrogen carbonate solution," *Bulletin of the Chemical Society of Japan*, vol. 63, no. 9, pp. 2459–2462, 1990.

[46] M. Azuma, K. Hashimoto, M. Hiramoto, M. Watanabe, and T. Sakata, "Carbon dioxide reduction at low temperature on various metal electrodes," *Journal of electroanalytical chemistry and interfacial electrochemistry*, vol. 260, no. 2, pp. 441–445, 1989.

[47] ——, "Electrochemical reduction of carbon dioxide on various metal electrodes in low-temperature aqueous khco 3 media," *Journal of the Electrochemical Society*, vol. 137, no. 6, pp. 1772–1778, 1990.

[48] A. Bewick and G. Greener, "The electroreduction of co2 to glycollate on a lead cathode," *Tetrahedron Letters*, vol. 11, no. 5, pp. 391–394, 1970.

[49] A. Aylmer-Kelly, A. Bewick, P. Cantrill, and A. Tuxford, "Studies of electrochemically generated reaction intermediates using modulated specular reflectance spectroscopy," *Faraday Discussions of the Chemical Society*, vol. 56, pp. 96–107, 1973.

[50] K. Ito, S. Ikeda, T. Iida, and H. Niwa, "Electrochemical reduction of carbon-dioxide dissolved under high-pressure. 2. in aqueous-solutions of tetraalkylammonium salts," *Denki Kagaku*, vol. 49, no. 2, pp. 106–112, 1981.

[51] M. Todoroki, K. Hara, A. Kudo, and T. Sakata, "Electrochemical reduction of high pressure co2at pb, hg and in electrodes in an aqueous khco3solution," *Journal of Electroanalytical Chemistry*, vol. 394, no. 1, pp. 199–203, 1995.

[52] F. Köleli, T. Atilan, N. Palamut, A. Gizir, R. Aydin, and C. Hamann, "Electrochemical reduction of co 2 at pb-and sn-electrodes in a fixed-bed reactor in aqueous k 2 co 3 and khco 3 media," *Journal of applied electrochemistry*, vol. 33, no. 5, pp. 447–450, 2003.

[53] Y. Akahori, N. Iwanaga, Y. Kato, O. Hamamoto, and M. Ishii, "New electrochemical process for co2 reduction to from formic acid from combustion flue gases," *Electrochemistry*, vol. 72, no. 4, pp. 266–270, 2004.

[54] T. E. Teeter and P. Van Rysselberghe, "Reduction of carbon dioxide on mercury cathodes," *The Journal of Chemical Physics*, vol. 22, no. 4, pp. 759–760, 1954.

[55] J. Jordan and P. Smith, "Free-radical intermediate in the electroreduction of carbon dioxide," pp. 246–247, 1960.

[56] A. Bewick and G. Greener, "The electroreduction of co2to malate on a mercury cathode," *Tetrahedron Letters*, vol. 10, no. 53, pp. 4623–4626, 1969.

[57] F. Wolf and J. Rollin, "Zur darstellung von äpfelsäure durch katodische reduktion von kohlendioxid," *Zeitschrift für Chemie*, vol. 17, no. 9, pp. 337–338, 1977.

[58] Y. Hori and S. Suzuki, "Electrolytic reduction of bicarbonate ion at a mercury electrode," *Journal of The Electrochemical Society*, vol. 130, no. 12, pp. 2387–2390, 1983.

[59] B. R. Eggins, E. M. Brown, E. A. McNeill, and J. Grimshaw, "Carbon dioxide fixation by electrochemical reduction in water to oxalate and glyoxylate," *Tetrahedron letters*, vol. 29, no. 8, pp. 945–948, 1988.

[60] S. Komatsu, T. Yanagihara, Y. Hiraga, M. Tanaka, and A. Kunugi, "Electrochemical reduction of co2 at sb and bi electrodes in khco3 solution," *Denki Kagaku*, vol. 63, no. 3, pp. 217–224, 1995.

[61] Y. Hori, A. Murata, R. Takahashi, and S. Suzuki, "Electroreduction of carbon monoxide to methane and ethylene at a copper electrode in aqueous solutions at ambient temperature and pressure," *Journal of the American Chemical Society*, vol. 109, no. 16, pp. 5022–5023, 1987.

[62] M. Fujihira and T. Noguchi, "A highly sensitive analysis of electrochemical reduction products of co2 on gold by new differential electrochemical mass spectroscopy (dems)." *Chemistry Letters*, no. 10, pp. 2043–2046, 1992.

[63] P. Kedzierzawski and J. Augustynski, "Poisoning and activation of the gold cathode during electroreduction of co 2," *Journal of The Electrochemical Society*, vol. 141, no. 5, pp. L58–L60, 1994.

[64] H. Noda, S. Ikeda, A. Yamamoto, H. Einaga, and K. Ito, "Kinetics of electrochemical reduction of carbon dioxide on a gold electrode in phosphate buffer solutions." *Bulletin of the Chemical Society of Japan*, vol. 68, no. 7, pp. 1889–1895, 1995.

[65] R. Shiratsuchi, S. Ishimaru, and G. Nogami, "Effects of surface structures of au electrodes on the pulsed electroreduction of co2," *Denki Kagaku Oyobi Kogyo Butsuri Kagaku*, vol. 66, no. 6, pp. 668–670, 1998.

[66] T. Ohmori, A. Nakayama, H. Mametsuka, and E. Suzuki, "Influence of sputtering parameters on electrochemical co2reduction in sputtered au electrode," *Journal of Electroanalytical Chemistry*, vol. 514, no. 1, pp. 51–55, 2001.

[67] R. Kostecki and J. Augustynski, "Electrochemical reduction of co2 at an activated silver electrode," *Berichte der Bunsengesellschaft für physikalische Chemie*, vol. 98, no. 12, pp. 1510–1515, 1994.

[68] N. Hoshi, M. Kato, and Y. Hori, "Electrochemical reduction of co2on single crystal electrodes of silver ag (111), ag (100) and ag (110)," *Journal of Electroanalytical Chemistry*, vol. 440, no. 1, pp. 283–286, 1997.

[69] H. Yano, F. Shirai, M. Nakayama, and K. Ogura, "Electrochemical reduction of co2at three-phase (gas liquid solid) and two-phase (liquid solid) interfaces on ag electrodes," *Journal of Electroanalytical Chemistry*, vol. 533, no. 1, pp. 113–118, 2002.

[70] A. Bandi, "Electrochemical reduction of carbon dioxide on conductive metallic oxides," *Journal of the Electrochemical Society*, vol. 137, no. 7, pp. 2157–2160, 1990.

[71] S. Ikeda, A. Hattori, K. Ito, and H. Noda, "Zinc ion effect on the electrochemical reduction of carbon dioxide at zincelectrode in aqueous solutions," *Denki Kagaku Oyobi Kogyo Butsuri Kagaku*, vol. 67, no. 1, pp. 27–33, 1999.

[72] W. M. Ayers and M. F. , *Electron Transfer Technologies Inc*, ser. ACS Symposium Series, Vol. 363. Princeton, NJ 08542, 1988, ch. 11, pp. 147–154.

[73] K. Ohkawa, K. Hashimoto, A. Fujishima, Y. Noguchi, and S. Nakayama, "Electrochemical reduction of carbon dioxide on hydrogenstoring materials: Part 1. the effect of hydrogen absorption on the electrochemical behavior on palladium electrodes," *Journal of Electroanalytical Chemistry*, vol. 345, no. 1, pp. 445–456, 1993.

[74] M. Azuma, K. Hashimoto, M. Watanabe, and T. Sakata, "Electrochemical reduction of carbon dioxide to higher hydrocarbons in a khco3aqueous solution," *Journal of electroanalytical chemistry and interfacial electrochemistry*, vol. 294, no. 1, pp. 299–303, 1990.

[75] K. Ohkawa, Y. Noguchi, S. Nakayama, K. Hashimoto, and A. Fujishima, "Electrochemical reduction of carbon dioxide on hydrogen-storing materials: Part 4. electrochemical behavior of the pd electrode in aqueous and nonaqueous electrolyte," *Journal of Electroanalytical Chemistry*, vol. 369, no. 1, pp. 247–250, 1994.

[76] B. Podlovchenko, E. Kolyadko, and S. Lu, "Electroreduction of carbon dioxide on palladium electrodes at potentials higher than the reversible hydrogen potential," *Journal of Electroanalytical Chemistry*, vol. 373, no. 1, pp. 185–187, 1994.

[77] H. Yoshitake, T. Kikkawa, and K.-i. Ota, "Isotopic product distributions of co2electrochemical reduction on a d flowing-out pd surface in protonic solution and reactivities of subsurface hydrogen," *Journal of Electroanalytical Chemistry*, vol. 390, no. 1, pp. 91–97, 1995.

[78] N. Hoshi, M. Noma, T. Suzuki, and Y. Hori, "Structural effect on the rate of co2 reduction on single crystal electrodes of palladium," *Journal of Electroanalytical Chemistry*, vol. 421, no. 1, pp. 15–18, 1997.

[79] C. Iwakura, S. Takezawa, and H. Inoue, "Catalytic reduction of carbon dioxide with atomic hydrogen permeating through palladized pd sheet electrodes," *Journal of Electroanalytical Chemistry*, vol. 459, no. 1, pp. 167–169, 1998.

[80] R. L. Cook, R. C. MacDuff, and A. F. Sammells, "High rate gas phase co 2 reduction to ethylene and methane using gas diffusion electrodes," *Journal of the Electrochemical Society*, vol. 137, no. 2, pp. 607–608, 1990.

[81] ——, "High rate gas phase co 2 reduction to ethylene and methane using gas diffusion electrodes," *Journal of the Electrochemical Society*, vol. 137, no. 2, pp. 607–608, 1990.

[82] K. Frese and S. Leach, "Electrochemical reduction of carbon dioxide to methane, methanol, and co on ru electrodes," *Journal of the Electrochemical Society*, vol. 132, no. 1, pp. 259–260, 1985.

[83] G. Arai, T. Harashina, and I. Yasumori, "Selective electrocatalytic reduction of carbon dioxide to methanol on ru-modified electrode." *Chemistry Letters*, no. 7, pp. 1215–1218, 1989.

[84] J. Qu, X. Zhang, Y. Wang, and C. Xie, "Electrochemical reduction of co2 on ruo2/tio2 nanotubes composite modified pt electrode," *Electrochimica Acta*, vol. 50, no. 16, pp. 3576–3580, 2005.

[85] D. P. Summers, S. Leach, and K. W. Frese Jr, "The electrochemical reduction of aqueous carbon dioxide to methanol at molybdenum electrodes with low overpotentials," *Journal of electroanalytical chemistry and interfacial electrochemistry*, vol. 205, no. 1, pp. 219–232, 1986.

[86] Y. Hori, K. Kikuchi, A. Murata, and S. Suzuki, "Production of methane and ethylene in electrochemical reduction of carbon dioxide at copper electrode in aqueous hydrogencarbonate solution," *Chemistry Letters*, no. 6, pp. 897–898, 1986.

[87] R. L. Cook, R. C. MacDuff, and A. F. Sammells, "On the electrochemical reduction of carbon dioxide at in situ electrodeposited copper," *Journal of The Electrochemical Society*, vol. 135, no. 6, pp. 1320–1326, 1988.

[88] O. Koga, K. Nakama, A. Murata, and Y. Hori, "Effects of surface-state of copper electrode on the selectivity of electrochemical reduction of carbon-dioxide," *Denki Kagaku*, vol. 57, no. 12, pp. 1137–1140, 1989.

[89] D. W. DeWulf, T. Jin, and A. J. Bard, "Electrochemical and surface studies of carbon dioxide reduction to methane and ethylene at copper electrodes in aqueous solutions," *Journal of The Electrochemical Society*, vol. 136, no. 6, pp. 1686–1691, 1989.

[90] S. Wasmus, E. Cattaneo, and W. Vielstich, "Reduction of carbon dioxide to methane and ethenean on-line ms study with rotating electrodes," *Electrochimica acta*, vol. 35, no. 4, pp. 771–775, 1990.

[91] A. Murata and Y. Hori, "Product selectivity affected by cationic species in electrochemical reduction of co2 and co at a cu electrode," *Bull. Chem. Soc. Jpn*, vol. 64, p. 123, 1991.

[92] K. W. Frese, "Electrochemical reduction of co2 at intentionally oxidized copper electrodes," *Journal of The Electrochemical Society*, vol. 138, no. 11, pp. 3338–3344, 1991.

[93] G. Kyriacou and A. Anagnostopoulos, "Electroreduction of co2 on differently prepared copper electrodes: The influence of electrode treatment on the current efficiences," *Journal of Electroanalytical Chemistry*, vol. 322, no. 1, pp. 233–246, 1992.

[94] ——, "Influence co2 partial pressure and the supporting electrolyte cation on the product distribution in co2 electroreduction," *Journal of applied electrochemistry*, vol. 23, no. 5, pp. 483–486, 1993.

[95] R. Shiratsuchi, Y. Aikoh, and G. Nogami, "Pulsed electroreduction of co2 on copper electrodes," *Journal of the Electrochemical Society*, vol. 140, no. 12, pp. 3479–3482, 1993.

[96] B. Jermann and J. Augustynski, "Long-term activation of the copper cathode in the course of co2 reduction," *Electrochimica acta*, vol. 39, no. 11, pp. 1891–1896, 1994.

[97] K. Hara, A. Tsuneto, A. Kudo, and T. Sakata, "Change in the product selectivity for the electrochemical co2 reduction by adsorption of sulfide ion on metal electrodes," *Journal of Electroanalytical Chemistry*, vol. 434, no. 1, pp. 239–243, 1997.

[98] P. Friebe, P. Bogdanoff, N. Alonso-Vante, and H. Tributsch, "A real-time mass spectroscopy study of the (electro) chemical factors affecting co2 reduction at copper," *Journal of Catalysis*, vol. 168, no. 2, pp. 374–385, 1997.

[99] Y. Terunuma, A. Saitoh, and Y. Momose, "Relationship between hydrocarbon production in the electrochemical reduction of co2and the characteristics of the

cu electrode," *Journal of Electroanalytical Chemistry*, vol. 434, no. 1, pp. 69–75, 1997.

[100] K. Ohta, K. Suda, S. Kaneco, and T. Mizuno, "Electrochemical reduction of carbon dioxide at cu electrode under ultrasonic irradiation," *Journal of the Electrochemical Society*, vol. 147, no. 1, pp. 233–237, 2000.

[101] J. Lee and Y. Tak, "Electrocatalytic activity of cu electrode in electroreduction of co2¡/sub¿," *Electrochimica acta*, vol. 46, no. 19, pp. 3015–3022, 2001.

[102] S. I. T. S. K. O. S. Kaneco, N. Hiei, *ITE Lett. Batt. New Technol. Med*, vol. 2, p. 83, 2001.

[103] Y. Hori, I. Takahashi, O. Koga, and N. Hoshi, "Selective formation of c2 compounds from electrochemical reduction of co2 at a series of copper single crystal electrodes," *The Journal of Physical Chemistry B*, vol. 106, no. 1, pp. 15–17, 2002.

[104] I. Takahashi, O. Koga, N. Hoshi, and Y. Hori, "Electrochemical reduction of co2 at copper single crystal cu and cu electrodes," *Journal of Electroanalytical Chemistry*, vol. 533, no. 1, pp. 135–143, 2002.

[105] H. Yano, F. Shirai, M. Nakayama, and K. Ogura, "Efficient electrochemical conversion of co2 to co, c2h4 and ch4 at a three-phase interface on a cu net electrode in acidic solution," *Journal of Electroanalytical Chemistry*, vol. 519, no. 1, pp. 93–100, 2002.

[106] Y. Momose, K. Sato, and O. Ohno, "Electrochemical reduction of co2 at copper electrodes and its relationship to the metal surface characteristics," *Surface and interface analysis*, vol. 34, no. 1, pp. 615–618, 2002.

[107] Y. Hori, I. Takahashi, O. Koga, and N. Hoshi, "Electrochemical reduction of carbon dioxide at various series of copper single crystal electrodes," *Journal of Molecular Catalysis A: Chemical*, vol. 199, no. 1, pp. 39–47, 2003.

[108] K. Ogura, H. Yano, and F. Shirai, "Catalytic reduction of co2 to ethylene by electrolysis at a three-phase interface," *Journal of The Electrochemical Society*, vol. 150, no. 9, pp. D163–D168, 2003.

[109] P. Dubé and G. Brisard, "Influence of adsorption processes on the co2 electroreduction: An electrochemical mass spectrometry study," *Journal of Electroanalytical Chemistry*, vol. 582, no. 1, pp. 230–240, 2005.

[110] Y. Hori, A. Murata, S.-y. Ito, Y. Yoshinami, and O. Koga, "Nickel and iron modified copper electrode for electroreduction of co2 by in-situ electrodeposition." *Chemistry Letters*, no. 9, pp. 1567–1570, 1989.

[111] A. Naitoh, K. Ohta, T. Mizuno, H. Yoshida, M. Sakai, and H. Noda, "Electrochemical reduction of carbon dioxide in methanol at low temperature," *Electrochimica acta*, vol. 38, no. 15, pp. 2177–2179, 1993.

[112] Y. Hori, A. Murata, and S.-Y. ITO, "Enhanced evolution of co and suppressed formation of hydrocarbons in electroreduction of co2 at a copper electrode modified with cadmium," *Chemistry Letters*, no. 7, pp. 1231–1234, 1990.

[113] G. Kyriacou and A. Anagnostopoulos, "Electrochemical reduction of co2 at cu+ au electrodes," *Journal of Electroanalytical Chemistry*, vol. 328, no. 1, pp. 233–243, 1992.

[114] M. Shibata and N. Furuya, "Simultaneous reduction of carbon dioxide and nitrate ions at gas-diffusion electrodes with various metallophthalocyanine catalysts," *Electrochimica acta*, vol. 48, no. 25, pp. 3953–3958, 2003.

[115] S. Ishimaru, R. Shiratsuchi, and G. Nogami, "Pulsed electroreduction of co 2 on cu-ag alloy electrodes," *Journal of The Electrochemical Society*, vol. 147, no. 5, pp. 1864–1867, 2000.

[116] R. Schrebler, P. Cury, F. Herrera, H. Gómez, and R. Córdova, "Study of the electrochemical reduction of co2 on electrodeposited rhenium electrodes

in methanol media," *Journal of Electroanalytical Chemistry*, vol. 516, no. 1, pp. 23–30, 2001.

[117] R. Schrebler, P. Cury, C. Suarez, E. Munoz, H. Gomez, and R. Cordova, "Study of the electrochemical reduction of co2 on a polypyrrole electrode modified by rhenium and copper–rhenium microalloy in methanol media," *Journal of Electroanalytical Chemistry*, vol. 533, no. 1, pp. 167–175, 2002.

[118] J. O. Bockris and S. U. Khan, *Surface Electrochemistry: A Molecular Level Approache*. Springer, 1993.

[119] K. Hara, A. Kudo, and T. Sakata, "Electrochemical reduction of carbon dioxide under high pressure on various electrodes in an aqueous electrolyte," *Journal of Electroanalytical Chemistry*, vol. 391, no. 1, pp. 141–147, 1995.

[120] ——, "Electrochemical reduction of high pressure carbon dioxide on fe electrodes at large current density," *Journal of Electroanalytical Chemistry*, vol. 386, no. 1, pp. 257–260, 1995.

[121] S. Kaneco, H. Katsumata, T. Suzuki, and K. Ohta, "Electrochemical reduction of co2 to methane at the cu electrode in methanol with sodium supporting salts and its comparison with other alkaline salts," *Energy & fuels*, vol. 20, no. 1, pp. 409–414, 2006.

[122] C. Amatore and J. M. Saveant, "Mechanism and kinetic characteristics of the electrochemical reduction of carbon dioxide in media of low proton availability," *Journal of the American Chemical Society*, vol. 103, no. 17, pp. 5021–5023, 1981.

[123] K. Ito, S. Ikeda, T. Iida, and A. Nomura, "Electrochemical reduction of carbon-dioxide dissolved under high-pressure. 3. in non-aqueous electrolytes," *Denki Kagaku*, vol. 50, no. 6, pp. 463–469, 1982.

[124] K. Ito, S. Ikeda, N. Yamauchi, T. Iida, and T. Takagi, "Electrochemical reduction products of carbon dioxide at some metallic electrodes in nonaqueous

electrolytes," *Bulletin of the Chemical Society of Japan*, vol. 58, no. 10, pp. 3027–3028, 1985.

[125] S. Ikeda, T. Takagi, and K. Ito, "Selective formation of formic acid, oxalic acid, and carbon monoxide by electrochemical reduction of carbon dioxide," *Bulletin of the Chemical Society of Japan*, vol. 60, no. 7, pp. 2517–2522, 1987.

[126] D. R. Lide, *CRC handbook of chemistry and physics*. CRC press, 2004.

[127] K. Binran, "The chemical society of japan," *Maruzen, Tokyo*, pp. 11–718, 1984.

[128] G. Hochgesand, "Rectisol and purisol," *Industrial & Engineering Chemistry*, vol. 62, no. 7, pp. 37–43, 1970.

[129] A. Naitoh, K. Ohta, T. Mizuno, H. Yoshida, M. Sakai, and H. Noda, "Electrochemical reduction of carbon dioxide in methanol at low temperature," *Electrochimica acta*, vol. 38, no. 15, pp. 2177–2179, 1993.

[130] ——, "Electrochemical reduction of carbon dioxide in methanol at low temperature," *Electrochimica acta*, vol. 38, no. 15, pp. 2177–2179, 1993.

[131] T. Mizuno, A. Naitoh, and K. Ohta, "Electrochemical reduction of co2 in methanol at- 30 c," *Journal of Electroanalytical Chemistry*, vol. 391, no. 1, pp. 199–201, 1995.

[132] H. Tributsch, J. Bockris, B. Conway, and R. White, "Modem aspects of electrochemistry, vol," 1986.

[133] S. Kaneco, K. Iiba, K. Ohta, T. Mizuno, and A. Saji, "Electrochemical reduction of co2 on au in koh+ methanol at low temperature," *Journal of Electroanalytical Chemistry*, vol. 441, no. 1, pp. 215–220, 1998.

[134] S. Kaneco, N.-h. Hiei, Y. Xing, H. Katsumata, H. Ohnishi, T. Suzuki, and K. Ohta, "High-efficiency electrochemical co2-to-methane reduction method using aqueous khco3 media at less than 273 k," *Journal of Solid State Electrochemistry*, vol. 7, no. 3, pp. 152–156, 2003.

[135] S. Kaneco, K. Iiba, M. Yabuuchi, N. Nishio, H. Ohnishi, H. Katsumata, T. Suzuki, and K. Ohta, "High efficiency electrochemical co2-to-methane conversion method using methanol with lithium supporting electrolytes," *Industrial & engineering chemistry research*, vol. 41, no. 21, pp. 5165–5170, 2002.

[136] S. Kaneco, K. Iiba, K. Ohta, and T. Mizuno, "Electrochemical reduction of carbon dioxide on copper in methanol with various potassium supporting electrolytes at low temperature," *Journal of Solid State Electrochemistry*, vol. 3, no. 7-8, pp. 424–428, 1999.

[137] S. Kaneco, K. Iiba, N.-h. Hiei, K. Ohta, T. Mizuno, and T. Suzuki, "Electrochemical reduction of carbon dioxide to ethylene with high faradaic efficiency at a cu electrode in csoh/methanol," *Electrochimica acta*, vol. 44, no. 26, pp. 4701–4706, 1999.

[138] S. Kaneco, K. Iiba, S.-k. Suzuki, K. Ohta, and T. Mizuno, "Electrochemical reduction of carbon dioxide to hydrocarbons with high faradaic efficiency in lioh/methanol," *The Journal of Physical Chemistry B*, vol. 103, no. 35, pp. 7456–7460, 1999.

[139] S. Kaneco, K. Iiba, K. Ohta, and T. Mizuno, "Reduction of carbon dioxide to petrochemical intermediates," *Energy Sources*, vol. 22, no. 2, pp. 127–135, 2000.

[140] Y. B. Vassiliev, V. Bagotsky, N. Osetrova, O. Khazova, and N. Mayorova, "Electroreduction of carbon dioxide: Part i. the mechanism and kinetics of electroreduction of co2 in aqueous solutions on metals with high and moderate hydrogen overvoltages," *Journal of Electroanalytical Chemistry and Interfacial Electrochemistry*, vol. 189, no. 2, pp. 271–294, 1985.

[141] K. Ito, S. Ikeda, and M. Okabe, "Reduction of carbon dioxide on partially immersed au plate electrode and au–spe electrode," *Denki Kagaku 48 (4): 247*, vol. 252, 1980.

[142] S. Nakagawa, A. Kudo, M. Azuma, and T. Sakata, "Effect of pressure on the electrochemical reduction of co2 on group viii metal electrodes," *Journal of electroanalytical chemistry and interfacial electrochemistry*, vol. 308, no. 1, pp. 339–343, 1991.

[143] A. Kudo, S. Nakagawa, A. Tsuneto, and T. Sakata, "Electrochemical reduction of high pressure co2 on ni electrodes," *Journal of The Electrochemical Society*, vol. 140, no. 6, pp. 1541–1545, 1993.

[144] K. Hara, A. Tsuneto, A. Kudo, and T. Sakata, "Shokubai 35 (1993) 513," in *Chem. Abstr*, vol. 120, 1994, p. 120149u.

[145] S. Nakagawa, A. Kudo, M. Azuma, and T. Sakata, "Effect of pressure on the electrochemical reduction of co2 on group viii metal electrodes," *Journal of electroanalytical chemistry and interfacial electrochemistry*, vol. 308, no. 1, pp. 339–343, 1991.

[146] A. Kudo, S. Nakagawa, A. Tsuneto, and T. Sakata, "Electrochemical reduction of high pressure co 2 on ni electrodes," *Journal of The Electrochemical Society*, vol. 140, no. 6, pp. 1541–1545, 1993.

[147] S. Kaneco, H. Katsumata, T. Suzuki, and K. Ohta, "Electrochemical reduction of carbon dioxide to ethylene at a copper electrode in methanol using potassium hydroxide and rubidium hydroxide supporting electrolytes," *Electrochimica acta*, vol. 51, no. 16, pp. 3316–3321, 2006.

[148] T. Mizuno, K. Ohta, M. Kawamoto, and A. Saji, "Electrochemical reduction of c02 on cu in 0.1 m koh-methanol," *Energy sources*, vol. 19, no. 3, pp. 249–257, 1997.

[149] H. Li and C. Oloman, "Development of a continuous reactor for the electroreduction of carbon dioxide to formate–part 1: Process variables," *Journal of Applied Electrochemistry*, vol. 36, no. 10, pp. 1105–1115, 2006.

[150] T. Mizuno, K. Ohta, A. Sasaki, T. Akai, M. Hirano, and A. Kawabe, "Effect of temperature on electrochemical reduction of high-pressure co2 with in, sn, and pb electrodes," *Energy Sources*, vol. 17, no. 5, pp. 503–508, 1995.

[151] H. Li and C. Oloman, "Development of a continuous reactor for the electro-reduction of carbon dioxide to formate–part 2: Scale-up," *Journal of Applied Electrochemistry*, vol. 37, no. 10, pp. 1107–1117, 2007.

[152] T. Yamamoto, D. A. Tryk, A. Fujishima, and H. Ohata, "Production of syngas plus oxygen from co2 in a gas-diffusion electrode-based electrolytic cell," *Electrochimica acta*, vol. 47, no. 20, pp. 3327–3334, 2002.

[153] K. Subramanian, K. Asokan, D. Jeevarathinam, and M. Chandrasekaran, "Electrochemical membrane reactor for the reduction of carbondioxide to formate," *Journal of applied electrochemistry*, vol. 37, no. 2, pp. 255–260, 2007.

[154] C. Delacourt, P. L. Ridgway, J. B. Kerr, and J. Newman, "Design of an electrochemical cell making syngas (co+ h2) from co2 and h2o reduction at room temperature," *Journal of The Electrochemical Society*, vol. 155, no. 1, pp. B42–B49, 2008.

[155] F. Bidrawn, G. Kim, G. Corre, J. Irvine, J. M. Vohs, and R. Gorte, "Efficient reduction of co2 in a solid oxide electrolyzer," *Electrochemical and Solid-State Letters*, vol. 11, no. 9, pp. B167–B170, 2008.

[156] Z. Zhan and L. Zhao, "Electrochemical reduction of co2 in solid oxide electrolysis cells," *Journal of Power Sources*, vol. 195, no. 21, pp. 7250–7254, 2010.

[157] S. D. Ebbesen and M. Mogensen, "Electrolysis of carbon dioxide in solid oxide electrolysis cells," *Journal of Power Sources*, vol. 193, no. 1, pp. 349–358, 2009.

[158] H. Yoneyama, K. Sugimura, and S. Kuwabata, "Effects of electrolytes on the photoelectrochemical reduction of carbon dioxide at illuminated p-type cadmium telluride and p-type indium phosphide electrodes in aqueous solutions,"

Journal of electroanalytical chemistry and interfacial electrochemistry, vol. 249, no. 1, pp. 143–153, 1988.

[159] E. E. Barton, D. M. Rampulla, and A. B. Bocarsly, "Selective solar-driven reduction of co2 to methanol using a catalyzed p-gap based photoelectrochemical cell," *Journal of the American Chemical Society*, vol. 130, no. 20, pp. 6342–6344, 2008.

[160] A. B. Bocarsly, Q. D. Gibson, A. J. Morris, R. P. LEsperance, Z. M. Detweiler, P. S. Lakkaraju, E. L. Zeitler, and T. W. Shaw, "Comparative study of imidazole and pyridine catalyzed reduction of carbon dioxide at illuminated iron pyrite electrodes," *ACS Catalysis*, vol. 2, no. 8, pp. 1684–1692, 2012.

[161] K. Nakaoka, J. Ueyama, and K. Ogura, "Photoelectrochemical behavior of electrodeposited cuo and cu2 o thin films on conducting substrates," *Journal of the Electrochemical Society*, vol. 151, no. 10, pp. C661–C665, 2004.

[162] K. Rajeshwar, N. R. de Tacconi, G. Ghadimkhani, W. Chanmanee, and C. Janáky, "Tailoring copper oxide semiconductor nanorod arrays for photoelectrochemical reduction of carbon dioxide to methanol," *ChemPhysChem*, vol. 14, no. 10, pp. 2251–2259, 2013.

[163] B. Conway and G. Jerkiewicz, "Relation of energies and coverages of underpotential and overpotential deposited h at pt and other metals to the volcano curvefor cathodic h2 evolution kinetics," *Electrochimica acta*, vol. 45, no. 25, pp. 4075–4083, 2000.

[164] S. Trasatti and H. Wendt, "Electrochemical hydrogen technologies," *Electrochemical hydrogen technologies*, 1990.

[165] A. J. Bard and L. R. Faulkner, *Electrochemical methods: fundamentals and applications*. Wiley New York, 1980, vol. 2.

[166] L. I. Bendavid and E. A. Carter, "Co2 adsorption on cu2o (111): A dft+ u and dft-d study," *The Journal of Physical Chemistry C*, vol. 117, no. 49, pp. 26 048–26 059, 2013.

[167] D. Canfield and K. Frese Jr, "Reduction of carbon dioxide to methanol on n- and p-gaas and p-inp: effect of crystal face, electrolyte and current density," *Journal of the Electrochemical Society*, vol. 130, no. 8, pp. 1772–1773, 1983.

[168] G. Ghadimkhani, N. R. de Tacconi, W. Chanmanee, C. Janaky, and K. Rajeshwar, "Efficient solar photoelectrosynthesis of methanol from carbon dioxide using hybrid cuo–cu 2 o semiconductor nanorod arrays," *Chemical Communications*, vol. 49, no. 13, pp. 1297–1299, 2013.

[169] Y. Zhou and J. A. Switzer, "Electrochemical deposition and microstructure of copper (i) oxide films," *Scripta materialia*, vol. 38, no. 11, pp. 1731–1738, 1998.

[170] A. Rakhshani and J. Varghese, "Surface texture in electrodeposited films of cuprous oxide," *Journal of Materials Science*, vol. 23, no. 11, pp. 3847–3853, 1988.

[171] A. Rakhshani, A. Al-Jassar, and J. Varghese, "Electrodeposition and characterization of cuprous oxide," *Thin Solid Films*, vol. 148, no. 2, pp. 191–201, 1987.

[172] L. Wang, N. De Tacconi, C. Chenthamarakshan, K. Rajeshwar, and M. Tao, "Electrodeposited copper oxide films: Effect of bath ph on grain orientation and orientation-dependent interfacial behavior," *Thin Solid Films*, vol. 515, no. 5, pp. 3090–3095, 2007.

[173] J. A. Switzer, M. G. Shumsky, and E. W. Bohannan, "Electrodeposited ceramic single crystals," *Science*, vol. 284, no. 5412, pp. 293–296, 1999.

[174] Y. Zhou and J. A. Switzer, "Electrochemical deposition and microstructure of copper (i) oxide films," *Scripta materialia*, vol. 38, no. 11, pp. 1731–1738, 1998.

[175] E. W. Bohannan, L.-Y. Huang, F. S. Miller, M. G. Shumsky, and J. A. Switzer, "In situ electrochemical quartz crystal microbalance study of potential oscillations during the electrodeposition of cu/cu2o layered nanostructures," *Langmuir*, vol. 15, no. 3, pp. 813–818, 1999.

[176] X. Jiang, T. Herricks, and Y. Xia, "Cuo nanowires can be synthesized by heating copper substrates in air," *Nano Letters*, vol. 2, no. 12, pp. 1333–1338, 2002.

[177] A. K. Hawley, H. M. Brewer, A. D. Norbeck, L. Paša-Tolić, and S. J. Hallam, "Metaproteomics reveals differential modes of metabolic coupling among ubiquitous oxygen minimum zone microbes," *Proceedings of the National Academy of Sciences*, vol. 111, no. 31, pp. 11 395–11 400, 2014.

[178] A. Cherashev and A. Khrushch, "The electrochemical reduction of carbon dioxide at the tin-cadmium and tin-zinc alloys," *Russian journal of electrochemistry*, vol. 33, no. 2, pp. 181–195, 1997.

BIOGRAPHICAL STATEMENT

Homayon Homayoni, M.S. is a Ph.D. student in Mechanical Engineering at the University of Texas at Arlington. He received a B.S. and M.S. in Mechanical Engineering in 2005 and 2008, respectively. His research involves the design and construction of reactors for the thermo-catalytic conversion of CO2 and CO to liquid fuels. He has worked on projects involving the conversion of coal to synthetic crude oil and natural gas to liquid fuels. His research also includes computational heat and mass transfer and computational fluid dynamics